Abstract

Introducing molecular properties into solid state devices is a step toward molecular electronics. I have investigated the effect of two series of ligands, di-sulfide and di-carboxylic ones, in which the substituent group can be, and is systematically changed. Quantitative FTIR spectroscopy shows that di-carboxylic ligands bind as carboxylate, to double surface sites. The binding constant increases with electron withdrawing power of the substituent, up to $3 \cdot 10^6$ M^{-1}. Di-sulfide ligands show two distinct stages of adsorption, viz. physisorption and chemisorption, with additional intra-layer bonding in the chemisorbed layer. Contact potential difference measurements reveal that adsorption increases electron affinity, reduces the band bending, and also decreases the rate of the decay of surface charge. The extent of change depends on the nature of both substituent and dipole groups. Correlation of the change in electronic properties with various molecular parameters reveals di-sulfide to have soft, polarizable interactions with the substrate, while di-carboxylic ligands have hard, localized interactions. Both reveal an acidic nature which decreases the surface charge of the substrate. The different interaction mechanism lead to different ways in which the molecular properties are expressed in electronic properties. The insight into ligand - semiconductor interactions gained by this work, may be utilized in the future for device applications.

Goals

To use the variability of adsorbed organic ligands to control the properties of GaAs(100) surface.

To this end we need to achieve the following:

1. Elucidation of the mode of chemisorption to aid in understanding the electronic effects of surface binding.
2. Measurement the of adsorbate-induced changes in electronic characteristics and determination of the relation between these changes and systematic variations in the adsorbate's properties.

1. Introduction

1.1 General:

The enormous versatility of organic molecules, fascinate many for their utilization in electronic devices. The functional complexity of biological molecules, together with the continued reduction in dimensions of electronic devices support the possibility of molecule-based electronics [1] The 'Grätzel cell' is the first successful example of a molecular electronic device where a molecular acceptor efficiently separates photoinduced charge for solar energy applications[2] Future emphasis will be on nanostructures that can gate electron currents[3].

In our group we try to graft molecular properties onto semiconductors with similar goals in mind. From the fundamental science point of view we use the molecules as a tool to understand semiconductor surface chemistry and physics. My study shows the possibility to bind certain classes of tailor-made organic molecules to GaAs surfaces, and to systematically modify the substrate properties by that. Combined with the highly developed processing technology of GaAs, this is a step towards the development of molecule-based electronic devices.

1.2 Semiconductor surfaces:

1.2.1 Surface states

The remarkable electronic and structural properties of semiconductor surfaces result from the existence of surface states. Intrinsic surface states originate from breaking of the lattice periodicity at the surface. Any additional atoms or molecules at the surface will modify the surface states by introducing new or modifying existing energy levels. Surface states with energy levels overlapping the bulk bands do not lead to charge localization, while surface states inside the forbidden gap can get charged. Then, due to charge neutrality, a space charge layer is formed.

1.2.2 Definitions

The common definitions are illustrated in figure 1. The Fermi level is the highest energy of electrons (or their electrochemical potential). Hence, at electronic equilibrium it must be equal all over the system, specifically, between the surface and the bulk. However occupation of surface states will lead to charge depletion in the semiconductor to preserve charge neutrality. The outcome is an electrical potential difference between the surface and the bulk, or the valence and conduction band positions differ at the surface and in the bulk. This is called band bending (BB). The potential (or energy) change as a function of the surface charge is called the space charge function F, and it can be found by solving the Poisson equation for the given charge density[4]. The work function (Φ) is defined as the difference in energy of an electron at rest in vacuum just outside and an electron at the Fermi energy inside the solid. Electron affinity (χ) is the difference between the vacuum level and the conduction band and ionization potential (I) is the energy difference to the valence band, all at the surface[4]. Changes in work function are the sum of electron affinity change and band bending change: $\Delta\Phi = \Delta\chi + \Delta\mathrm{BB}$. In general, electron affinity changes are due to dipole changes, while band bending changes are due to variations in surface charge distribution.

1.2.3 Surface dipole moment

Adsorption of foreign molecules modifies the surface dipole moment by their own 'built-in' dipole moment; by the adatom-surface bond itself due to differences in electronegativites; or by merely changing the surface reconstruction. In the case of GaAs, changes in reconstruction and surface stoichiometry can induce dipole moment changes of more than 1 eV, without any adsorption. Hence the exact surface chemistry is directly translated into physical properties by altering the distribution of surface states and the dipole moment at the surface[4].

Provided the respective dipoles posses components normal to the surface ($p_\perp$), an electric double layer will form. Depending on the direction of the respective dipole moment, the voltage drop across the electronic double layer leads to an increase or a reduction of electron affinity (χ) of an initially clean surface by:

$$\Delta\chi = \pm\frac{1}{\varepsilon_o}\cdot p_\perp(\theta)\cdot N_{ad} \qquad (1.1$$

where N_{ad} is the number of adsorbate-induced surface dipoles per unit area; and ε_o is the permitivity of vacuum. The dipole moment $p_\perp(\theta)$ itself decreases as a function of coverage θ, since each dipole is exposed to the electrostatic field of all other dipoles which is in the opposite direction. The depolarization of the dipoles is given by: $p_d(\theta) = 4\pi\varepsilon_o\alpha_{ad}\cdot E_d(N_{ad})$ (1.2

where α_{ad} is the polarizability of the adsorbates. At any dipole site, the total depolarizing electric field (E_d) of all other surrounding dipoles is obtained by summing over all the neighboring dipoles, which is coverage dependent. The variation in electron affinity finally results as:

$$\Delta\chi = \pm\frac{1}{\varepsilon_o}\cdot\frac{p_\perp\cdot N_{ad}}{1+9\alpha_{ad}N_{ad}^{3/2}} \qquad (1.3$$

where the factor of 9 fits for hexagonal surface symmetry.

1.2.4 Surface band bending

With increasing density of surface states, the band-bending initially changes very rapidly, but it saturates for higher densities of surface states This behavior is commonly referred to as pinning of the Fermi level. The equilibrium band bending can be changed by injecting charge into the space charge layer. This can be done by an external electric field or by illumination. The absorption of light with photon energies larger than the bulk band gap generates electron-hole pairs. The electric field of the space charge layer spatially separates the injected electron-hole pairs and thereby reduces the space charge, i.e. the bands are flattened. This effect is called surface photovoltage, and it is used to measure the band bending by comparing the surface potential at equilibrium (dark) and under saturation illumination[4]. A major drawback for this method are the surface traps which may equilibrate only very slowly with the bulk[5] Many papers report time scales of minutes to hours[6,5,7] to recover the dark CPD. Bednyi relates this to the large concentration of minority carriers under illumination,

which result in a different space charge function (Q_{ss} vs. BB) relative to the dark space charge function. The minority carriers are produced very fast by illumination, but recombine slowly due to surface traps, in the light to dark transition. This excess photoinduced surface charge will manifest itself as a small (fast) change in BB under illumination, and as a large (slow) change in BB in the dark. Some theoretical treatment is possible for the simpler case of one type of surface state, but it becomes very complicated for a combination of hole and electron traps at the surface.

1.2.5 Experimental surface study

Historically, there have been two approaches to study solid surfaces: in solution (electrochemistry) and in UHV. Working in solution allows one to use more 'real' systems, while working in UHV gives well-defined surfaces and reactions. However, it is difficult to extrapolate UHV information to real systems[3]. The ambient-pressure contact-less Kelvin probe method used here, represents an intermediate approach between the solution and UHV approaches. Between the numerous surface techniques, photoemission to measure ionization potential, and photoluminescence for measuring BB and surface recombination velocity are widely used alternatives to the Kelvin probe used here.

1.3 Adsorption:

1.3.1 Basic phenomena

Binding of an adsorbate to the surface, as well as the action of the adsorbate-surface complex, involves charge transfer from the substrate to the molecule or vice versa. Miller et. al. mention three key concepts in understanding electron transfer at surfaces: 1) the energy of the interacting levels; 2) the nuclear modes that define the reaction coordinate; and 3) the electronic coupling between the discrete molecular orbitals and the energy bands of the surface states. For a dry, directly bound adsorbate, the dominant factor is the electronic coupling to the surface or, in other words, the overlap of the unperturbed orbital with surface states, and the magnitude of charge redistribution required for efficient overlap[3,8].

The adsorption strength of large organic molecules on the surface of a semiconductor is related to several different attractive forces and degree of charge-sharing between the adsorbate and the substrate[3]. Charge transfer originates from quantum mechanical interactions, which are much less understood than electromagnetic interactions that are involved in electric, optical or magnetic phenomena. Quantum mechanical interactions refer to intermediate distances. They are neither the short 'bonding' distances, nor the long, intermolecular force distances, and basic theory is still unsatisfactory[1].

Few models to understand the interaction of ligands with the surface have been suggested, including acid-base interactions[8], uncompleted valences [9], and a molecular orbital approach[10,4]. They represent different aspects of the phenomena, and will be reviewed shortly.

1.3.2 Acid-base description

In the acid-base description the surface is classified as an acid (electron acceptor) or a base (electron donor) according to the direction of the net electron transfer which results in the formation of the chemical bond with an adsorbate molecule. Net electron transfer from the surface (base) to the adsorbate (acid) increases the work function and vice versa. For metal surfaces, due to the continuum of filled and empty states, the surface has no intrinsic acid-base character and it depends only on the adsorbate. In some instances also semiconductor surfaces can have both types of states, acidic (acceptor) or basic (donor). The degree of coupling between the molecule and the surface can be viewed in terms of hard and soft acid-base interactions[8]. Delocalized surface states will react stronger with π orbitals. In contrast to σ bonds (e.g. COO^-) that would be stabilized by the presence of localized acidic sites[8].

1.3.3 Free valence description

Wolkenstein emphasizes the free valences at the surface as the interaction entities. Free electrons or holes can be regarded as 'free valences', i.e. one less (hole) or one more (electron) for a complete shell, respectively. A free surface valence is involved in a strong bonding, and the valence becomes localized and bound to the adsorbate particle. In weak bonding there is no charge transfer from the lattice, which means that the energy of the bonding electrons is in the conduction band, i.e. they are delocalized. At equilibrium, the reactivity of the chemisorbed particle is uniquely determined by the position of the Fermi level, by its control over electron and hole concentration at the surface. Thus by moving the Fermi level we can change the nature of the bonding from weak to strong. The Fermi level is therefore a regulator of a variety of surface properties such as the reactivity of the surface, charging of adsorbed particles, weak or strong binding, and the ratio between adsorption and desorption[9].

1.3.4 Molecular orbital description

The molecular orbital description is based on electronic interactions between molecular and surface energy states that leads to a splitting into two states with an energy difference that is twice the electronic interaction energy. The molecule interacts via its HOMO or LUMO depending on its base (donor) or acid (acceptor) properties, respectively. The resulting filled and empty (bonding and anti-bonding) states change the energy distribution of the surface states. The energy levels of the ligand are relatively simple to get from the literature or by calculation, but the surface energy levels are much more complicated to predict. They can be related to the lattice atoms, e.g. as sp^3 dangling hybrid orbitals for diamond structure materials[4], or to a distinct 'unknown' surface phase or to unknown surface defects[10], [11]. Mɣnche's approach is supposed to be more predictive, using electronegativities, but the results are only qualitatively correct and limited to adsorption of mono-valent atoms.

The molecular orbital approach seems to be the most precise of the three, however it deals only with the basic parameter of the energetics [3], which is not sufficient for complete description. The other two approaches are trying to account for orbital's overlap (soft / hard interactions) or the resulting charge transfer (weak-strong binding).

1.4 GaAs surfaces:

GaAs is a compound semiconductor with zinc blende (diamond) structure, with a room temperature direct band gap of 1.42 V. In this work I study the GaAs (100) surface, which is the one most frequently used for device applications. The work function of GaAs(100) surfaces varies as a function of their reconstruction, and thereby, surface composition, from 4.6 V to 5.15 V [Monch]. For GaAs (100), irrespective of the type of reconstruction, the Fermi level is obviously pinned at approximately 0.5±0.1 eV above the valence-band maximum. Pinning is due to a sufficiently large density of surface states of both donor and acceptor type (both n- and p- types are pinned)[4]. A summary of surface electronic properties of GaAs is given in appendix 6. The GaAs crystals were highly n-type doped ($N_D > N_C$). Therefore it is reasonable to assume that the Fermi level nearly coincides with the conduction band.

1.5 Passivation of GaAs surfaces:

The passivation of GaAs surfaces is one of the key problems in III-V semiconductor device technology The desirable properties of a passivating overlayer are: the terminating phase is covalently bound to the surface; it has a wider band gap than the substrate; and its formation eliminates substrate dangling bonds without introducing new states within the forbidden gap[12]. In contrast to silicon, where SiO_2 produces a perfect electronic interface, oxidation of GaAs does not improve its electronic properties and results in an unstable surface oxide, with activation energy for oxide dissolution of the order of 20 kJ/mol. Oxygen uptake is stimulated by exposure to photons with sufficient energy to generate electron-hole pairs[4].

Sandroff and Yablonovitch were the first to use inorganic sulfur for GaAs surface passivation[13]. Since then extensive research was done to improve the efficiency and stability of the sulfur treatment, to investigate its mechanism, and to explore the resulting surface phases, especially in terms of oxides and sulfur bonding to As, Ga or both. Sulfur was adsorbed from $Na_2S \cdot 9H_2O$, $(NH_4)_2S$ or $(NH_4)_2S_x$ aqueous solutions. Sulfide chemical treatment showed improvements in some simple electronic devices, mainly by decreasing the surface recombination velocity[14].

There have been at least two models used to explain the passivation phenomenon: one proposes a sulfide induced surface charge that repels electrons away from recombination sites at the surface, and the other proposes a reduction of As vacancies and As antisite defects which have a midgap energy level, thus reducing the recombination center density. Whatever the mechanism for passivation, improved device performance has been well documented, but the problem of the stability of the resulting surface towards light, air, temperature, and water rinsing remains[15]. Other inorganic passivations include H_2S treatment[16], NH_4F[17], $P_2S_5/(NH_4)_2S$[18], electrochemical sulfur deposition[15] and chemical vapor deposition of GaS from $[(t\text{-}Bu)GaS]_4$[19].

1.6 Adsorption to semiconductor surfaces - Work outside WIS:

Self assembled monolyers (SAM) are well known to form on oxide (SiO_2) and coinage metal substrates. Two groups have investigate the formation of alkyl-thiol SAMs on GaAs (100). Allara and coworkers studied the packing of alkyl-thiol SAM's on (100) GaAs. They found a stable, highly organized assembly of conformationally ordered, tilted alkyl chains, chemically bonded directly to the bare GaAs surface, with high stability toward oxidation. They did not give any information about the binding mechanism[20]. The group of Allara could not produce a di-sulfide SAM, although they were able to do so on gold. Asai et. al. succeeded to adsorb amphiphilic disulfides ($[CH_3(CH_2)_{17}]_2NCSS$ Na) on GaAs (100), with some passivating effect[21]. Nakagawa et. al. studied the electrical properties of a Schottky diode with metal contact evaporated on top of the octadecyl-thiol SAM, by IV and CV measurements. They found that the SAM modifies the Schottky barrier height up to 40 meV. PL measurements didn't show a significant intensity change. Apparently both the effective surface recombination velocity and the surface state density were unaffected by the passivation[22]

The group of Ellis did extensive work on the change in surface electronic properties as a result of adsorption of simple organic molecules on CdS and CdSe surfaces. They used series of aniline derivatives as Lewis bases and carbonyl compounds as Lewis acids and measured the PL signal in solution. Their major results were that bases 'push' electrons from their HOMO to the surface states, and therefore increase the band bending (for an n-type semiconductor), while acids, acting through their LUMO can stabilize the surface states of a semiconductor, trapping additional charge at the surface and expanding the depletion region. Only modest changes in surface recombination velocity were measured. Binding constants vary over four orders of magnitude, with electron withdrawing substituents stabilizing the binding, consistent with a Lewis acidic

interaction with the surface that is Lewis basic. Adduct stability is enhanced by resonance effects. No correlation was found between the amount of PL quenching with any molecular property. Correlation with Hammett parameter was found for the binding constant of two types of ligands, but not for another two types[10].

N. Lewis and co-workers investigated adsorption of thiols and other Lewis bases on GaAs (100), by PL measurements. Effective coordination to the recombination site was found to be an important component of improving the PL signal. Sulfide influence was much larger than that of amines or alcohols, suggesting that the surface site is "soft" in character, and prefers polarizable ligands. This would fit an electron deficient site, such as As°, or possibly Ga atoms in GaAs lattice, but is not consistent with expectations for an oxide type acceptor site. Exposure of the surface to organic thiols didn't yield detectable XPS signals for an As_2S_3 phase, which was found for inorganic sulfur treatments. The lack of XPS evidence may be due to the very small number of reconstruction sites which is below the XPS detection level[11].

These result indicates that effective passivation of GaAs surface recombination can occur without gross changes in surface stoichiometry. However, it also implies that effective binding to the important chemical recombination sites is required, and that S donors are substantially more effective than "harder", less polarizable, O and N bases. The important recombination sites act as soft, polarizable, electron deficient centers[11,23].

1.7 Adsorption to semiconductor surfaces - Work in WIS:

In the group of David Cahen research of molecular modifications of electronic properties of semiconductor surfaces started with simple molecules such as para-substituted benzoic acids. The substituent group allows systematic investigation of molecular interaction with different substrates such as CdTe, CdSe, $CuInSe_2$ and GaAs. The benzoic acids were found to bind as carboxylate to the cation in the compound semiconductor, and to induce a substantial dipole moment on the surface. The direction and strength of the dipole depends on the para-substituent, and revealed a linear correlation to the ligands dipole moment. Electron withdrawing substituents such as a nitro group increase the work function, while electron donating ones, such as a methoxy group, decrease the work function between 0.4 V to 1V depending on the substrate. Also the binding strength was a function of the substrate, and seems to correlate with the ionicity of the substrate[24].

After demonstrating the feasibility of dipole modification by molecular adsorption, more advanced, 'tailor made' ligands were used. A set of benzo-hydroxamic acids on CdTe and $CuInSe_2$ induced a change in electron affinity of 550 up to 670 mV[25]. Because they failed to affect the band bending, ligands with other binding groups were synthesized. Di-sulfide ligands that are known to bind to Au have been tried too. On CdTe and $CuInSe_2$ they affect the electron affinity and the band bending to a small degree[26]. Finally, the effective binding of benzoic acids led to synthesis of di-carboxylic acids which allows more flexibility of functional groups, and is supposed to bind stronger. Indeed, di-carboxylic ligands adsorbed on CdTe, show for the first time substantial changes in the band bending up to 400 mV (~70%), in addition to the change in electron affinity of about 400 mV[27].Initial results now indicate the possibility of using these molecular modified properties in devices. One approach was to produce a heterojunction cell with adsorbed molecules incorporated into it. Substantial changes were observed in the IV characteristics of $CuIn(Ga)Se_2$ / CdS devices for different di-carboxylic ligands adsorbed at the interface[28]. Another direction was to use the ligands to gate the current in a GaAs transistor (FET or HEMT configuration). Ligands were found to decrease the current substantially, and slow the relaxation time of the photocurrent by three orders of magnitude. Moreover, the relaxation time was sensitive to the ligands' resonance wavelength (I was involved directly in this project)[29]. This clearly indicates translation of a molecular property into a solid state device. To gain more understanding and control over these ligand - substrate interactions, I investigated adsorption of two families of tailor-made ligands: the di-carboxylic and di-sulfides, on GaAs, chemically by the FTIR-ATR technique, and electronically by the Kelvin probe method (contact potential difference measurements).

2. Experimental Methods.

2.1 Infrared - ATR measurements

2.1.1 Infrared spectroscopy

Chemical information about the binding of the ligands to the GaAs surface was obtained from infrared (IR) spectroscopy. IR is a vibrational spectroscopy, and as such it is sensitive to chemical environment, but less characteristic of elemental composition. This is useful for gaining information about the chemical state of adsorbed molecules and their orientation. Difficulties in quantitative analysis are due to overlap of different absorption bands, and absorption dependence on various factors like orientation, and induced electric field.

A vibrational mode will be IR-active if during the vibration there is a change in dipole moment, which interacts with the electric field of the radiation. Therefore, asymmetric vibrational modes and vibrations due to polar groups are the ones most likely to exhibit prominent IR adsorption. The IR spectrum is obtained by plotting the absorbance versus the IR energy, usually in units of wavenumber [cm^{-1}]. In Fourier Transform IR (FTIR) the beam has a wide wavenumber range which is later decomposed mathematically into its components by Fourier transformation. This shortens considerably the scanning time and allows better resolution and signal to noise ratio. The availability of fast Fourier transform (FFT) expands significantly the application of IR spectroscopy and enables measuring very small quantities[30].

2.1.2 Application of FTIR to surfaces:

The study of binding thin molecular films to a surface can be done with various IR accessories. Eliminating the powder techniques (Diffuse reflectance etc.), because we are interested in single crystals, we have three options: direct transmittance, external reflectance or internal reflectance. Transmittance is the common mode for IR spectroscopy where the beam passes through the sample. It can be used if the substrate (GaAs) has relatively low absorbance and the system is sensitive enough to the small quantities of surface adsorbates. In external reflectance (sometimes called Reflection-Absorbance, or grazing angle) the beam comes in at a high angle to the sample normal (80°-88°) and reflects back to the detector. This technique is most appropriate to metals or opaque substrates. Because the beam is almost parallel to the surface, it detects only the vibrational component perpendicular to the substrate surface. By combining transmittance and grazing

angle measurements the tilt and packing of molecules can be found[31,32,33]. I have tried these two techniques on GaAs without much success, although they work well with thin films of $CuInSe_2$ on glass[34] and with Si wafers[35]. It is still left to the future to find the right conditions to apply these IR modes to GaAs.

Internal reflectance is usually known as ATR (Attenuated Total Reflectance) or sometimes MIR (Multiple Internal Reflectance). In this technique the infrared beam goes through a high refractive index crystal having low bulk absorption in the infrared region. Generally the crystal geometry is a parallelepiped and the beam enters at an angle to the crystal plane, so that total reflection occurs inside the crystal (see figure 2). In general, the crystal (high refractive index) / air (low refractive index) interface is totally reflecting, and a standing wave perpendicular to it is formed. If the sample absorbed some of the radiation, the propagating wave interacts with the sample and becomes attenuated. The reflectance (R) is:

$$R^N = \left(1 - a \cdot d_e\right)^N \qquad (2.1)$$

where N is the number of reflections, d_e is the effective layer thickness, and a is the absorptivity. The amplitude of the electric field, E, falls off exponentially with the distance:

$$E = E_o \cdot \exp\left(\frac{-z}{d_p}\right) \qquad (2.2)$$

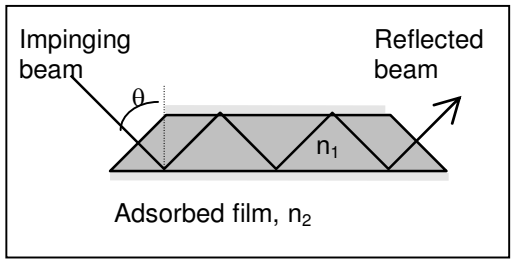

Figure 2: Scheme of use of ATR method for FT-IR.

where z is the distance from interface into the film, and d_p is the typical depth of penetration and depends on the refractive indices of the crystal (n_1) and sample (n_2), the impinging angle with the surface normal (θ) and the wavelength inside the crystal (λ_o):

$$d_p = \frac{\lambda_o}{2\pi n_1}\left(\sin^2\theta - \frac{n_2}{n_1}\right)^{-1/2} \qquad (2.3)$$

From equations 2.2 and 2.3 we can see that radiation at long wavelengths (low wavenumbers) penetrates deeper than at short ones, so that the ATR spectra are not linear with the wavenumber. This is very important for quantitative measurements and comparison between different IR techniques. It also can be seen that the penetration decreases with θ and n_1 (n_1 can be changed by crystal type and doping).

Although the studied film can be adsorbed on to any substrate, which later is pressed to the ATR crystal[31], this is not recommended due to surface roughness on the order of the penetration depth for ATR (4

nm to 3 μm)[32]. The main disadvantage in adsorbing directly on the ATR crystal arises from the need to keep the ATR surface as perfect as possible. Therefore we avoid any surface treatments, such as etching or polishing and adsorb on a rather oxidized surface, unlike the conditions for samples measured in the Kelvin probe.

Immersion of an ATR crystal in the adsorbing solution enables real time monitoring of the adsorption process dynamics, following the energy shifts and intensity changes for characteristic peaks[32]. I could not use this method because a liquid ATR cell was not available to me. Other workers were able to follow adsorption kinetics with 'dry' ATR[31]. As a compromise, I extracted data about adsorption kinetics by static measurements of dry samples, after immersion in different concentrations, for constant duration. The required immersion time was determined by following the signal intensity (i.e. adsorption rate) for a single concentration.

2.1.3 Experimental details

All IR spectra were taken using a Bruker IFS66 FTIR in the ATR mode. The ATR crystal was undoped GaAs(100) with edge angle of 45° and 10 cm² surface area (2′1′5). The crystal was purchased from Harrick Co. Considerations, and specific conditions of the FTIR operation appears in appendix 1.

The background reference spectrum was taken just before adsorption. For isotherms, the reference was taken only once at the beginning of the set, and the whole set was accomplished within 6-8 hr. From time to time the signal intensity was checked to assure that no big deviations occurred.

Working in the range of 1700-1000 cm^{-1} requires extensive purging of water vapor from the chamber, by continuous flow of N_2. Spectra were collected until a minimum water signal was measured. Further purging will result in 'negative' water peaks (relative to the background).

As shown in the results part, the only efficient cleaning of the ATR crystal was boiling methanol for 20 - 30 min. The ATR crystal was cleaned before any adsorption, and the crystal was kept as much as possible covered with either methanol or adsorbing solution.

For adsorption the crystal was kept in a 30 ml glass vial under ambient conditions, with adsorption duration noted in the results. Adsorption solutions for isotherms were freshly made by dilution of one initial solution. The procedure of calculating surface coverage from the raw IR spectra is described in appendix 2.

2.2 Kelvin Probe Measurements

2.2.1 The Kelvin probe method for CPD measurements

The work function of the modified surfaces was measured by the Kelvin probe (KP) method, which is illustrated in figure 3. In this method the work function is calculated from the contact potential difference (CPD) between the unknown sample and a reference which is the vibrating probe. The KP method does not use a front contact to the surface and therefore bypasses some of the major difficulties in surface electronic measurement. It is applicable to a wide range of temperatures and pressures, and easy to apply. The measured work function is an arithmetic mean, which is useful for rejecting small disturbances, but makes the measurement slow and quite sensitive to environment noise[36].

Lord Kelvin was the first (1898) to notice that the CPD at one particular junction can be distinguished from all other circuit junctions by changing the distance between the surfaces, thus affecting junction capacitance. Zisman[37] (1932) was the first to use a vibrating electrode, and Brattain and Bardeen (1953) applied it to semiconductor (Ge) surface measurements[4]. Today, modified forms of KP have developed as surface photovoltage spectroscopy (SPS)[38] and KP microscopy combined with AFM[39].

Any two electronically connected materials will equilibrate their Fermi levels. However, each one of them has a different work function. Thus the local vacuum level (i.e. the energy of an electron just outside the range of image forces of the material) will be different between them. This difference is the CPD and shown schematically in figure 2.a.[37, 40]. This phenomenon is applied in KP by vibrating one of the surfaces, at frequency ω, resulting in a periodically varying capacitance. The scheme of the method is shown in figure 2.b. The specimen and the vibrating probe form two electrodes of a capacitor C. They are connected through a resistor R, ammeter, and controlled DC source V_b. In zero current condition, the backing voltage V_b is equal in magnitude and opposite in sign to the CPD, as explained next.

Between the sample and the probe there is a net field of V = CPD + V_b. Changing the capacitance C will change the charge Q and hence a current (i) will flow through the back contact:

$$i = \frac{\partial Q}{\partial t} = \frac{\partial (C \cdot V)}{\partial t} = V \frac{\partial C}{\partial t} \qquad (2.4)$$

(assuming the net voltage is constant). The capacitance depends on the electrode area (A), the dielectric constant (ε), and the distance between the electrodes (d): $C = A/\varepsilon d$. In the KP method the capacitance is changing as a result of changing the distance d by the vibrating electrode. The probe is vibrating sinusoidal by a piezoelectric driven mechanism, hence:

$$i = \frac{VA}{\varepsilon} \cdot \frac{\partial}{\partial t}\left(\frac{1}{d_o + a \cdot \sin(\omega t)}\right) \propto \frac{VA}{\varepsilon d_o} \cos(\omega t) \qquad (2.5)$$

(Actually this is only the first term of a solution in the form of Fourier series, but the higher terms are negligible)[40]. From equation 2.5 it is clear that with no voltage across the capacitor (V= CPD + V_b =0), no current will flow in the circuit. Therefore the backing voltage V_b is a direct measurement of the CPD, provided the current is zero.

CPD measurements were done using a Besocke delta phi commercial setup[41]. It uses a gold grid of 2 mm diameter as the probe driven by a piezoelectrical mechanism. An electronics box generates the signal to vibrate the piezo, measure the output current, and apply a feedback loop to null the current, i.e. to control the backing voltage. The feedback dictates the time response of the system. For this setup the vibration frequency is ~200 Hz and the fastest time constant of the feedback is 0.1 second. The box allows monitoring the signal shape on an auxiliary scope (the 'zero current' is never really zero) and output to record the applied backing voltage , i.e. the CPD.

In our setup CPD data were collected via a Keithley digital voltmeter, with GPIB output connected to a PC. A simple C program originally written by Leonid Chernyak and modified by me was used for this purpose. The program is given in appendix 7. It allows overnight measurements with adjustable time resolution from 0.1 sec to a few hours; time intervals can be changed during the measurement; and the accumulated data vs. time is shown on the computer screen.

The sample and the probe are held in a closed metallic box to screen electrostatic noise. A 360 W halogen lamp with concentrator lens was used to flatten the surface band bending. The back contact to the GaAs sample was made with InGa, to the base of the box which was connected to earth.

2.2.2 Noise problems in KP measurements

At the beginning of the work, severe problems of reproducibility arose in KP measurements. Together with Dr. Stephane Bastide we tried to identify the reasons for it. The prime findings were that KP results depends strongly on the surrounding humidity and on the mean distance between the sample and the probe. The humidity effect is probably due to water vapor condensation on both the probe and the sample, which acts to alter their work function, and the resulting CPD by up to 200 mV. This problem was solved by surrounding the metal measuring box with a non-permeable plastic bag filled with argon. This has a significant influence on CPD results as shown in figure 9.

Theoretically, the KP probe is indifferent to the mean probe to sample separation, because current nulling depends solely on the voltage. Practically, all capacitor parameters like area and distance (mean and amplitude) do have a great influence on the signal to noise ratio, hence changing these parameters varies the noise part of the reading[42]. Therefore the way to reduce the distance dependence is to reduce the overall noise. Working with a commercial setup most of the noise problems are solved by the manufacturer. The major noises we considered were electrostatic[43],[44], microphonics and amplification[42]. With the help of Eng. Reuven de Roos, improved cables and connections were used. Later a number of measurements were taken to define the amplification conditions which are the least sensitive to distance variations. The final result was a change of 10 mV over a 500 μm distance change. Despite these significant improvements, the reproducibility for GaAs measurements was around ±40 mV error in Ar dry bag and ~±100 mV in air. This is probably due to the very reactive and unstable GaAs surface.

2.3 Adsorbed ligands

Two families of ligands were compared in this work, as shown in figure 4. One type is based on tartaric acid as the binding group, and the other binds through a dithiane part; they are called di-carboxylic and di-sulfide respectively. For each binding base two arms of 'dipole' groups were connected via an ester. Mostly symmetric forms were used, with both arms of the same substituted phenyl, but in a few cases, one of the phenyls was replaced by a 15 carbon alkyl chain.

The following terminology is used: the first two letters refer to the dipole group and the last letters to the binding group. Hence DHDC stands for di-**h**ydrogen di-**c**arboxylic, and MODS stands for mono-meth**o**xy di-**s**ulfide (with C_{15} alkyl on the other arm). Other substituents include: Cyano (**C**), methyl (**M**), di-methyl amine (**N**), and tri-fluoro methyl (**F**). Table 1 summarize the studied ligands and their abbreviations:

Table 1: List of ligands used in this study:

Code	Binding	R1	R2	name
DCDC	Tartaric acid	Cyano - **C**N	Cyano - **C**N	p-cyano benzene
MCDC	Tartaric acid	Cyano - **C**N	alkyl $(CH_2)_{14}CH_3$	" + palmitol
DFDC	Tartaric acid	tri Fluoro methyl C**F**$_3$	tri Fluoro methyl C**F**$_3$	p-trifluoro methyl
DHDC	Tartaric acid	Hydrogen - **H**	Hydrogen - **H**	benzene
DMDC	Tartaric acid	**M**ethyl - CH_3	**M**ethyl - CH_3	toluene
MODC	Tartaric acid	methoxy - **O**CH_3	alkyl $(CH_2)_{14}CH_3$	anisol + palmitol
DCDS	diThiane	Cyano - **C**N	Cyano - **C**N	p-cyano benzene
MCDS	diThiane	Cyano - **C**N	alkyl $(CH_2)_{14}CH_3$	" + palmitol
DNDS	diThiane	di methyl amin-**N**$(CH_3)_2$	di methyl amin-**N**$(CH_3)_2$	aniline
DODS	diThiane	methoxy - **O**CH_3	methoxy - **O**CH_3	anisol
MODS	diThiane	methoxy - **O**CH_3	alkyl $(CH_2)_{14}CH_3$	anisol + palmitol

Ligands were synthesized by the group of Avi Shanzer. These specific ligands were originally developed for work with Au, CdTe and $CuInSe_2$.

2.4 Sample preparation and adsorption procedure

Sample preparation for GaAs wafers is a standard technique in general. The first stage is usually degreasing of the sample after shelf storage. This is done by sequential rinsing and sonicating in organic solvents and water, which should dissolve a wide range of possible contaminants. The second step of etching differs between the various research groups. Etching is usually done to remove the natural oxide from the surface. GaAs, a compound semiconductor, has different reactivities of As and Ga (or their oxides) towards different reagents: therefore different etches leave different surface stoichiometries and surface roughnesses. The most common etch is the 'sulfuric etch', H_2SO_4:H_2O_2:H_2O in ratios ranging from 8:1:1 to 1:8:500. The first composition relates to diffusion controlled etching which is very vigorous and acts to polish the surface, while the second composition is reaction rate limited, and is much more gentle. The peroxide oxidizes the surface, and the acid complexes the oxide and dissolves it. Also base can be used to dissolve the oxide and it was reported that high pH etchants protect the more soluble Ga by hydroxyl binding to it. Therefore basic etchants are found to give a more stoichiometric surface than acid ones. A common basic etch is bromine -methanol solution for oxidation, followed by KOH immersion to remove the oxide. XPS measurements showed Br/MeOH etching to give better stoichiometry and less residual oxide than sulfuric etch[24]. One disadvantage of Br/MeOH etching was that often it leaves the surface spotty, because it is a reaction controlled etching. This problem was solved by adding a polishing step before the etching that removes all previous surface damages. This was especially important for the re-use of samples where previous treatments left considerable damage to the surface.

Commercial GaAs wafers were purchased from American Xtal Technology. Wafers were (100) oriented, Si - n doped with N_d = 0.7 - 1 10^{18} cm^{-3}, and resistivity of 1.6 - 3 10^{-3} Ω·cm.

The wafers were cut to pieces of ~1،1 cm^2. Used samples were immediately cleaned by 1M KOH to remove the InGa back contact, then boiled in methanol for ~20 min to remove the previously adsorbed ligands, and kept for further use.

Degreasing was done by successive stages of boiling in trichloroethylene, sonicating in acetone and in methanol for ~5 min each step. Polishing was done by H_2SO_4:H_2O_2:H_2O - 3:1:1 v/v for 30 sec and running deionized water rinsing for another 30 sec. Samples were kept immersed in methanol (analytical grade). To avoid oxidation as much as possible, further treatment and measurements were done inside a dry bag filled with

filtered argon. Etching was done by three repeated 15 sec immersing in Br_2-methanol (0.05 % (v/v) Br_2 : methanol) and 1M KOH, with fast dip into methanol and water between them. Immediately after the etching the sample was rinsed with acetonitrile and put into the adsorbing solution. To eliminate oxidation as much as possible, CPD measurement of the as-etched sample was avoided.

A solution of 0.5 mM ligands in acetonitrile was prepared in the dry bag just before adsorption. Methanol and acetonitrile were extra dry grade, although the 'dry bag' includes water from the etching stage. Thus it was not dry, but rather oxygen free. High argon pressure was kept to prevent air leakage inside.

Samples were immersed in the adsorbing solution overnight (14-20 hr) and then transferred to the KP dry bag (without any water) for CPD measurement. Each sample was measured 3 times: as taken out from the solution, and after a fast dip into pure acetonitrile for two times. The excess solvent was Ar blown dry inside the bag. For each ligand 3-4 samples were prepared, hence a total of 9-12 data sets were collected. The averaged results were calculated from the 5-7 data points that showed best consistency.

3. Results

3.1 FTIR-ATR

FTIR-ATR was used to investigate the chemistry of ligand adsorption, in terms of the type of chemical bonding, adsorption time for equilibrium, stability toward rinsing, and approximate binding curves. Four representative ligands were investigated , two with the carboxylic- and two with the dithiane-binding group, two with an electron-withdrawing functional group (DCDC, DCDS) and two with an electron-donating functional group (DHDC, DODS). Binding curves were measured for all of these except DODS.

3.1.1 Analysis of spectra for the bound complex

Figure 5 shows a comparison between the bound complex and the free ligand, for the four ligands . The bound complex was measured on a GaAs ATR crystal as described in the experimental part, and the free ligands were measured by Dr. Merlin Bruening (DCDS, DODS) and Rami Cohen (DCDC, DHDC) in the transmittance mode, using a KBr pellet. The KBr spectra show minor interactions between the ligands and the KBr (fig. 5.a, ν_{S1}), and may be in the future the use of another medium, such as nujol is more appropriate for this purpose.

Our main interest is in the binding group, i.e. the change in chemical state of the carboxylic and dithiane groups. The carboxylic absorption bands ($\nu_{(C=O)}$, $\nu_{(C-O)}$) are very strong and any change in electron distribution (e.g. hydrogen bonding, or metal binding) is observed as an energy shift of the peaks. Especially the ionic (COO^-) form is characterized by disappearance of the original peaks at ~1700 cm^{-1} ($\nu_{(C=O)}$) and ~ 1270 cm^{-1} ($\nu_{1(C-O)}$) due to electron resonance on both oxygens, resulting in an asymmetric stretch at ~1640 (ν_{s1}) and a symmetric stretch at ~1400 cm^{-1} (X_1). The S-S or S-metal bands are all out of our detection range (the GaAs ATR crystal absorbs IR radiation below ~500 cm^{-1}) [30]. Following is a comparison between the major bands (represented by dotted lines on fig. 5) for the four ligands.

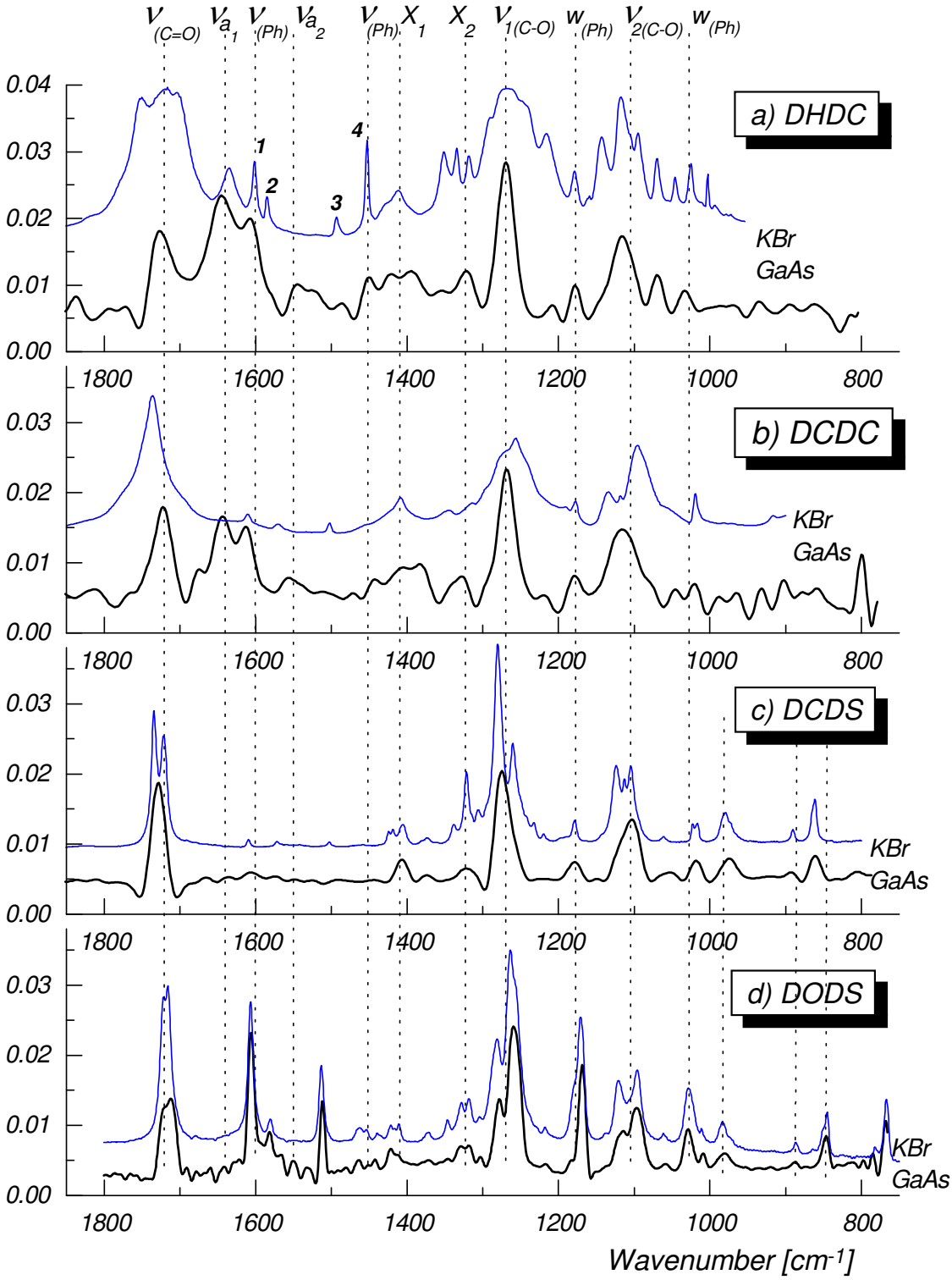

Figure 5: Peak identification for adsorbed and free ligands.
a) DHDC; b) DCDC; c) DCDS; d) DODS.
Arbitrary absorption units.

Carbonyl stretching at ~1730 cm^{-1}($\nu_{(C=O)}$).

This peak is clearly changed for the di-carboxylic ligands from the free ligand to the adsorbed form. The bound state shows a single, relatively sharp peak from the ester group, in contrast to the broad peaks in the KBr spectrum. This indicates that the carboxylic carbonyl disappears and the adsorbed molecules are not in their acidic form, but rather in ionic-carboxylate form as discussed in the next section.

For both free and bound di-sulfides a single peak is expected due to the ester carbonyl. For the free (KBr) ligand there is a strong split in DCDS and a smaller one for DODS. This can be explained by dimerization between free ligands, or some in-layer (hydrogen) bonding for the bound di-sulfide. Upon adsorption the splitting disappears for DCDS and remains for DODS. I assume that this is due to different adsorption duration (DCDS after ½ hr, and DODS after 20 hr), and not because of different molecular properties. The DODS spectrum after 4 hr adsorption (shown in fig 6.b.) looks more like the DCDS, than as the DODS after 20 hr. It seems that the splitting indicates additional bonding[30] (inside the layer, or bonding to a second layer) and represents higher order in the adsorbed layer that requires prolonged adsorption. The exact nature of the bonding is unknown. Although there is no direct evidence for the changes in di-sulfide spectrum upon adsorption, it seems that stable binding can be detected by the splitting in $\nu_{(C=O)}$ and $\nu_{1(C-O)}$ as will be discussed below.

Carboxylate modes - (ν_{s1}, ν_{s2}, X_1, X_2):

The carboxylate form of the adsorbed carboxylic acid (5.a, 5.b) is indicated by new peaks in the spectrum, which do not exist for the free [45,24]. Indeed, for both DHDC and DCDC there is a clear asymmetric band at 1644 cm^{-1}(ν_{a1}), and a weaker peak at 1550 cm^{-1} (ν_{a2}). The clusters marked by X_1 and X_2 are changed. The area of 1300 - 1400 cm^{-1} which includes X_1 and X_2 is very difficult to interpret because it can relate to deformation modes of hydrogen on the α carbons of the ligand. However the change can be due to additional symmetric stretch of the carboxylate. Obviously, none of these bands appears for the di-sulfides. The IR results show clearly that di-carboxylic ligands adsorb to the surface as carboxylates. The two asymmetric and probably two symmetric peaks indicate that the carboxylate exists in two different binding environments, something that will be considered further in the discussion section 4.1.2.

C-O stretching ($\nu_{1(C-O)}$, $\nu_{2(C-O)}$).

For di-carboxylic acids, the 1270 cm^{-1} band ($\nu_{1(C-O)}$) is broad in KBr because of contributions from the acid and from the ester C-O stretching, while in the bound form only the ester absorbs and the peak becomes sharper. With di-sulfides in KBr, we find an unexpected splitting, with opposite intensities for DODS and DCDS. Similarly to what we saw for the $\nu_{(C=O)}$ band, upon adsorption the splitting disappears for DCDS and remains for DODS. This can simply support the previous explanation, but it also could be due to a C-S stretching mode, which is expected at ~1290 cm^{-1}[30]. This explanation is not very likely because the splitting vanishes upon adsorption of DCDS. The C-S stretching might be weak and covered by the C-O stretching, or it might be shifted to higher energy (around X_2).

Finally, the 1120 band ($\nu_{2(C-O)}$) is attributed to the aryl conjugated ester[30], and bands that change upon adsorption could be seen in that range for all four ligands, except for DODS, which keeps the same splitting as in KBr. Therefore the C-O stretching behaves similar to the C=O stretching and its behaviour supports the previous conclusion, of absence of the acidic form for the adsorbed di-carboxylic ligands, and occurrence of some new bonding of the ester group in stable adsorbed di-sulfide.

Benzene ring modes (ν_{ph}, w_{ph}):

Another group of bands is due to benzene ring vibrations. It is subdivided into C-C deformations (ν_{ph}:1610 - 1400 cm^{-1}), with four distinct peaks (marked by 1-4 in the upper spectrum of fig. 5.a.), and in benzene hydrogen bending peaks (w_{ph}:1200 - 900 cm^{-1}) which are more ambiguously assigned[30]. The intensity of the benzene carbon stretching (ν_{ph}) is much higher for electron donating substituents (DHDC, DODS), than for electron withdrawing substituents (DCDC, DCDS). As the electron distribution on the two para substituents (carbonyl on one side and CN, OMe etc. on the other side) becomes more alike, the ring stretching signal will diminish, because symmetrical stretches are not observed in IR. Another explanation could be that the cyano substituent drastically reduces the electron distribution in the benzene ring, and hence, the signal intensity. Anyway, the benzene carbon modes are clear demonstration for the large molecular changes imposed by the substituent.

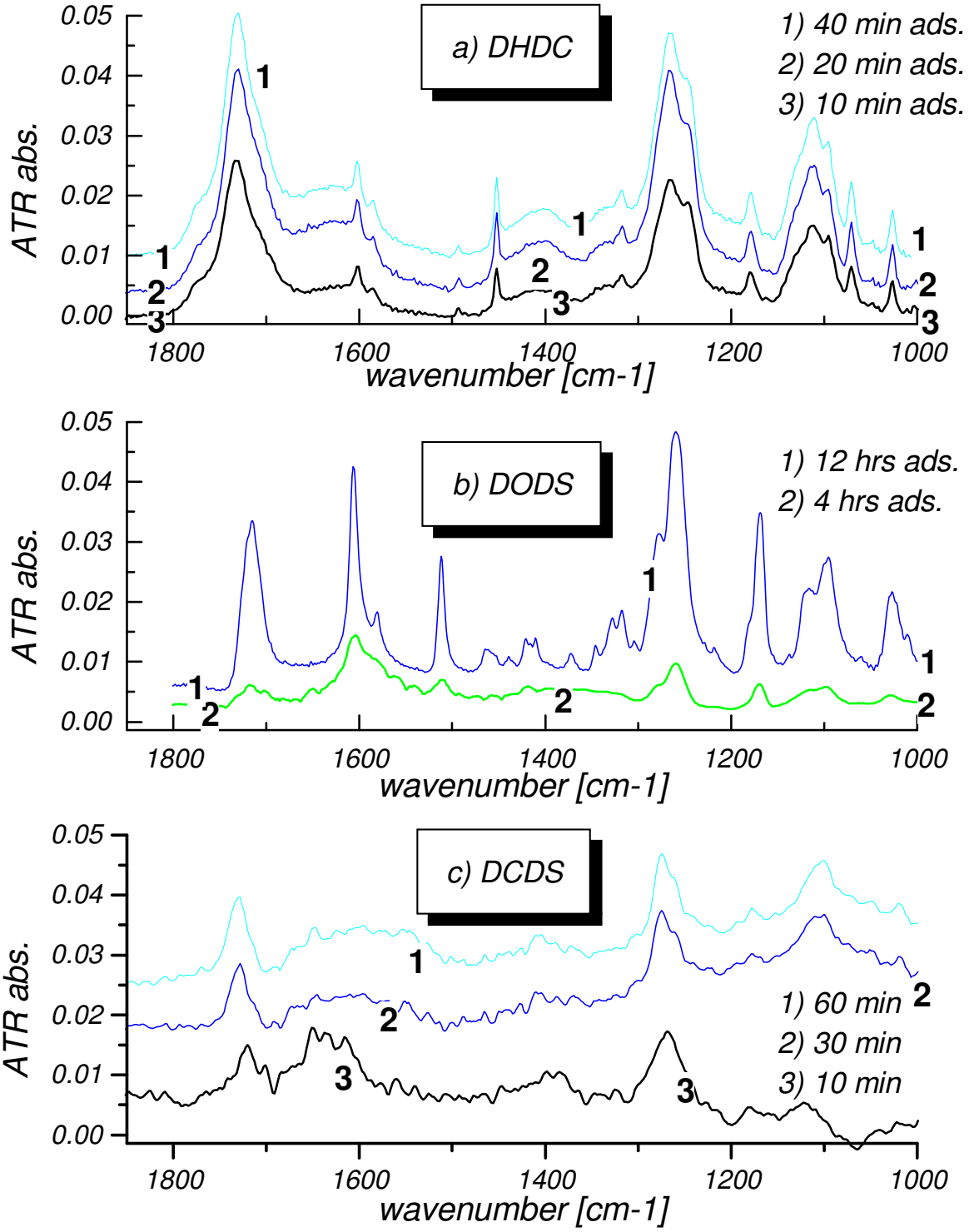

Figure 6: Comparing IR signal intensity for different adsorption duration a) DHDC; b) DODS; c) DCDS.

Benzene hydrogen wagging modes (w_{ph}) are probably responsible for the clear 1180 and 1020 cm^{-1} bands, which are characteristic for these ligands. For di-sulfides, the dithiane hydrogen modes are probably seen in the 1420 cm^{-1} area. Below 900 cm^{-1} there are peaks in the same position for all di-sulfide spectra that can be fitted to the dithiane catalog spectrum[46].

3.1.2. Stability of the bound layer

To verify the proper conditions for stable layer formation I measured the signal change due to adsorption time, and the stability of the layer toward rinsing with neat solvent. The results are presented in figures 6 and 7, respectively.

Fig. 6.a shows the spectrum of adsorbed DHDC on the GaAs - ATR crystal after adsorption for 10, 20, and 40 min., at a concentration of 1.1 mM. There is some increase in signal between 10 and 20 min., but from 20 to 40 min. the signal is nearly identical. As shown in fig. 7.a. after this short adsorption (40 min.) the adsorbed layer is very stable toward rinsing, except for the small excess that is washed away in the first rinse. Similar results for rinsing are obtained with DCDC and shown in fig. 7.b. Hence a layer obtained after 30 min. adsorption layer can be regarded as a stable equilibrium layer. I assume similar behavior for other di-carboxylic ligands.

For DODS the sample was measured after 4 hr adsorption, then put into the adsorbing solution for another 20 hr and measured again. The intensity of the peaks increased significantly and vibrational bands are much more distinct and clear after 20 hr. DCDS was measured only for short duration. However, the small differences between the spectra (fig 6.c.) led me to the wrong conclusion that one hour adsorption period is enough to get a stable layer. Comparison of figure 6.b. and 6.c. clearly shows that the short adsorption time of DCDS looks more like the short adsorption of DODS and not the stable 20 hr DODS adsorption. Moreover, the 20 hr adsorption is fairly stable against rinsing as shown in figure 7.d, while the 1 hr adsorbed DCDS layer is washed away easily. Also the 4 hr DODS is washed away easily. This suggest that di-sulfides need prolonged adsorption time to produce stable, ordered layers. Otherwise they are probably only physisorbed on the surface. This realization fits with reported high temperature used to adsorb thiols[20].

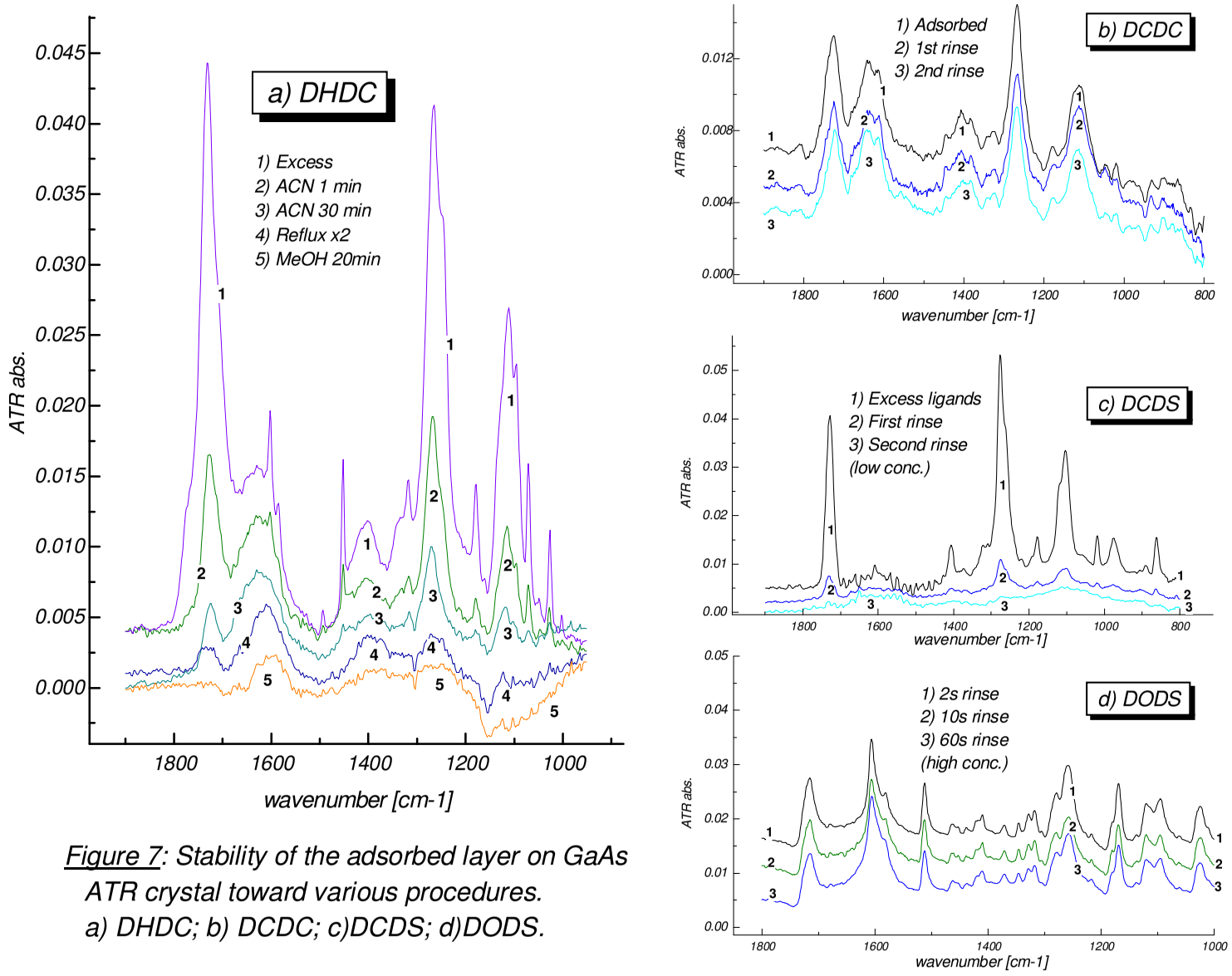

Figure 7: Stability of the adsorbed layer on GaAs ATR crystal toward various procedures. a) DHDC; b) DCDC; c)DCDS; d)DODS.

With di-carboxylic ligands, the opposite problem arose, i.e. I couldn't remove the ligands from the surface. Even severe measures such as hot acetonitrile for 30 min., boiling chloroform for 20 min., followed by 40 min. isopropanol reflux, applied twice, didn't remove the IR ligand bands, as shown in figure 7.a. The only efficient treatment was boiling methanol, after which little of the absorption spectrum remained, although the 1600 band still remains. It might be due to methanol binding or ligand fractions. The success of methanol cleaning can be understood by considering its ability to complex oxidized Ga and As[47]. Obviously, a stronger etchant will remove the ligands, but destroy the ATR surface at the same time. DODS after 20 hr adsorption was quite stable with various acetonitrile rinses, and eventually was removed by 1 hr immersion in cold methanol.

.1.3 Binding curves

To be able to obtain a more quantitative comparison of binding strength, I made a set of binding curves for three ligands: DHDC, DCDC, and DCDS. The GaAs ATR crystal was immersed in adsorption solution for sufficiently long time to give equilibrium adsorption, except for DCDS, which later was found to be far from equilibrium. Equilibrium adsorption for di-sulfides requires ~1 day for each isotherm point (or heating) which is a little impractical. Thus the DCDS results that are shown refer to physi- rather than chemisorption.

Figure 8.a gives the results in direct form. The errors are calculated from 5-6 different vibrational bands for each ligand, as described in appendix 2.

For a first approximation, I assumed the simplest adsorption conditions, namely one binding site per molecule. For Langmuir isotherms there is a linear relation between reciprocal coverage and concentration: $\frac{1}{\theta} = 1 + \frac{1}{K \cdot C}$ and these are shown in figure 8.b. The results are clearly non-linear, and this suggests the binding mechanism involves two binding sites per molecule. The Langmuir isotherm for this case is presented as a quadratic relation between coverage (θ) and concentration (C): $\frac{\theta}{(1-\theta)^2} = K \cdot C$. This is shown in figure 8.c. These results show that physisorption of the di-sulfide fits better to a single adsorption site (8.b.) while di-carboxylic adsorption fits to two binding sites (8.c.). The lines in figure 8.a. are calculated by these fits.

The use of Langmuir isotherms allows us to extract from the data the binding constant (K) and to approximate the coverage without an independent calibration spectrum (see appendix 2). As seen in the figure, DCDC is closer to a complete monolayer than DHDC, and its binding constant is about 10 times bigger than the binding constant for DHDC. DCDS barely covers half the surface, and is only physisorbed to the surface.

The binding constant K is directly related to the binding energy by: $-\Delta G = k_B T \cdot \ln K$. Table 2 summarizes the measured binding constants and calculated energies, for the three ligands investigated here, and compares the observed values to those of some representative samples from the literature.

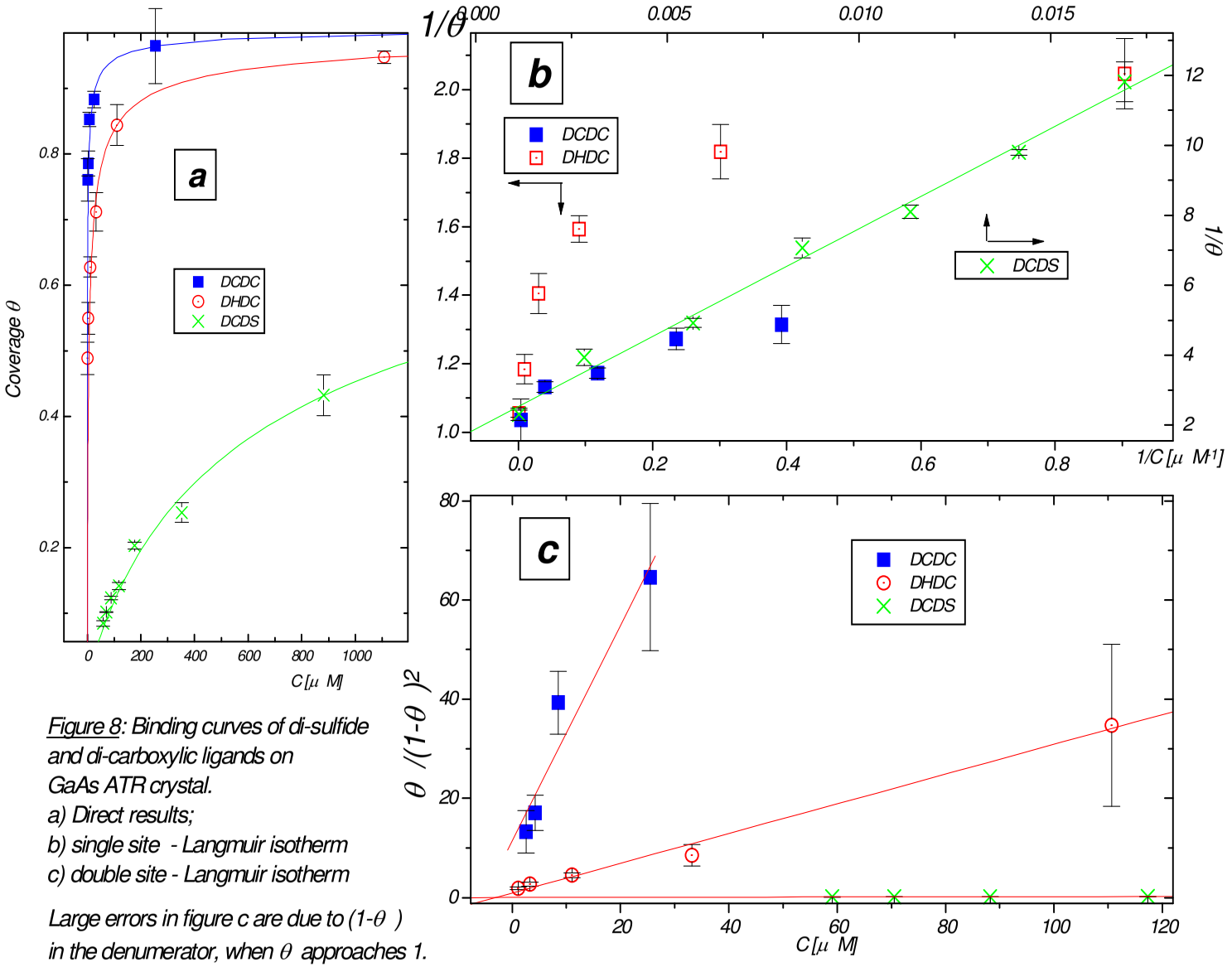

Figure 8: Binding curves of di-sulfide and di-carboxylic ligands on GaAs ATR crystal.
a) Direct results;
b) single site - Langmuir isotherm
c) double site - Langmuir isotherm

Large errors in figure c are due to (1-θ) in the denumerator, when θ approaches 1.

Table 2: Binding constants and energies for ligands adsorbed on semiconductors:

Ligand	substrate	K 10^4 [M^{-1}]	-ΔG [kJ/mol]	Method
DCDC	GaAs	300	37.2	ATR-FTIR
DHDC	GaAs	31	31.5	ATR-FTIR
DCDS	GaAs	0.17	18.6	ATR-FTIR
DHDS[48]	CdTe	1.6	24.1	Powder
DH - hydroxamic acid[48]	CdTe	0.40	20.7	Powder
Benzoic acid[24]	GaAs	0.21	24.8	ATR-FTIR
Benzoic acid[49]	CdTe	0.13	17.8	ATR-FTIR
Benzoic acid[49]	ZnSe	0.63	21.8	ATR-FTIR
Benzealdehyde[10]	CdS(e)	0.1	17.2	PL
di keton di phenyl[10]	CdS(e)	3	25.7	PL
quinone[10]	CdS(e)	20	30.4	PL

Summary of infrared results:

Infrared spectroscopy reveals di-carboxylic ligands to form a carboxylate complex with the surface. There is no evidence concerning the sulfur state of adsorbed di-sulfides, but long adsorption duration results in intra-layer bonding of the carbonyl group. Di-carboxylic molecules reach equilibrium adsorption after 20-30 min., while the rate of di-sulfide adsorption was much slower, more than 4 hours. Rinsing with acetonitrile removes excess of molecules from the layer, but has no influence on the stable layer, for both di-carboxylic and di-sulfide ligands. Di-carboxylic binding isotherms show double site adsorption, with stronger binding of DCDC than DHDC. No reliable isotherm was obtained for di-sulfides.

3.2 Contact potential difference - CPD

Evaluation of the electronic interaction between the ligands and the GaAs surface was done by measuring the effect of the ligands on the surface potential.. Samples were measured using the Kelvin probe method under argon (unless otherwise specified) in the dark and under illumination. The results summarize the molecule-induced changes for dark and light 'steady state' and the time- and light intensity-dependent behavior.

3.2.1 Surface pre-treatment:

Various etching treatments were tried, and the results are summarized elsewhere[24]. They indicate Br/methanol + KOH etching to be the most appropriate etchant. The effects of this etchant are shown in figures 9.c and 9.d. together with the results of a sulfuric acid etchant (9.a) which is supposed to leave the surface with excess As°. Also shown is the result of treatment with ammonium sulfide, which is known to have a passivating effect on GaAs [14]. [12](applied after initial sulfuric acid etching). Curves 9.a - 9.c are done in air and 9.d was measured inside an argon filled dry bag.

Figure 9 demonstrates the general form of data collected and the influence of different etchants. All measurements start in the dark until a stable value is reached. This value is taken as the dark work function, or bent band WF. The sharp decrease in WF is due to sample illumination which excites electron-hole pairs and flattens the bands. The extent of band flattening, or 'light saturation' is checked by increasing the light intensity in 3-4 steps, as can be seen in Fig. 9. Saturation is reached if the CPD value is constant with increasing light intensity. As shown in fig. 9, I couldn't reach photo-saturation for treatment a and b. For curve c the result is more satisfactory (illumination was a little stronger). As a result, we used a higher power lamp (360W instead of 300W). Even with the more intense illumination (fig 9.d) the CPD did not reach complete saturation. Further increase in light intensity and duration was restricted because of severe heating of the system, suspected to damage the sample[45], or to burn the bag. The spikes seen in fig 9.a and 9.d are due to overshoots in the electronic feedback control, which cannot follow the very fast CPD changes. They are good indicators for fast response, but not related to charge transfer at the sample surface. Finally we consider the rising part of the curve, i.e. the rate at which the system returns to its dark equilibrium value after illumination. Ammonium sulfide treatment (9.b) causes much faster return to the dark than Br-methanol, which is faster in air (9.c) than in argon (9.d). This is attributed to enhanced passivation of the $(NH_4)_2S$ treatment. Further discussion of equilibrium recovery for the ligands is given in section 3.2.4.

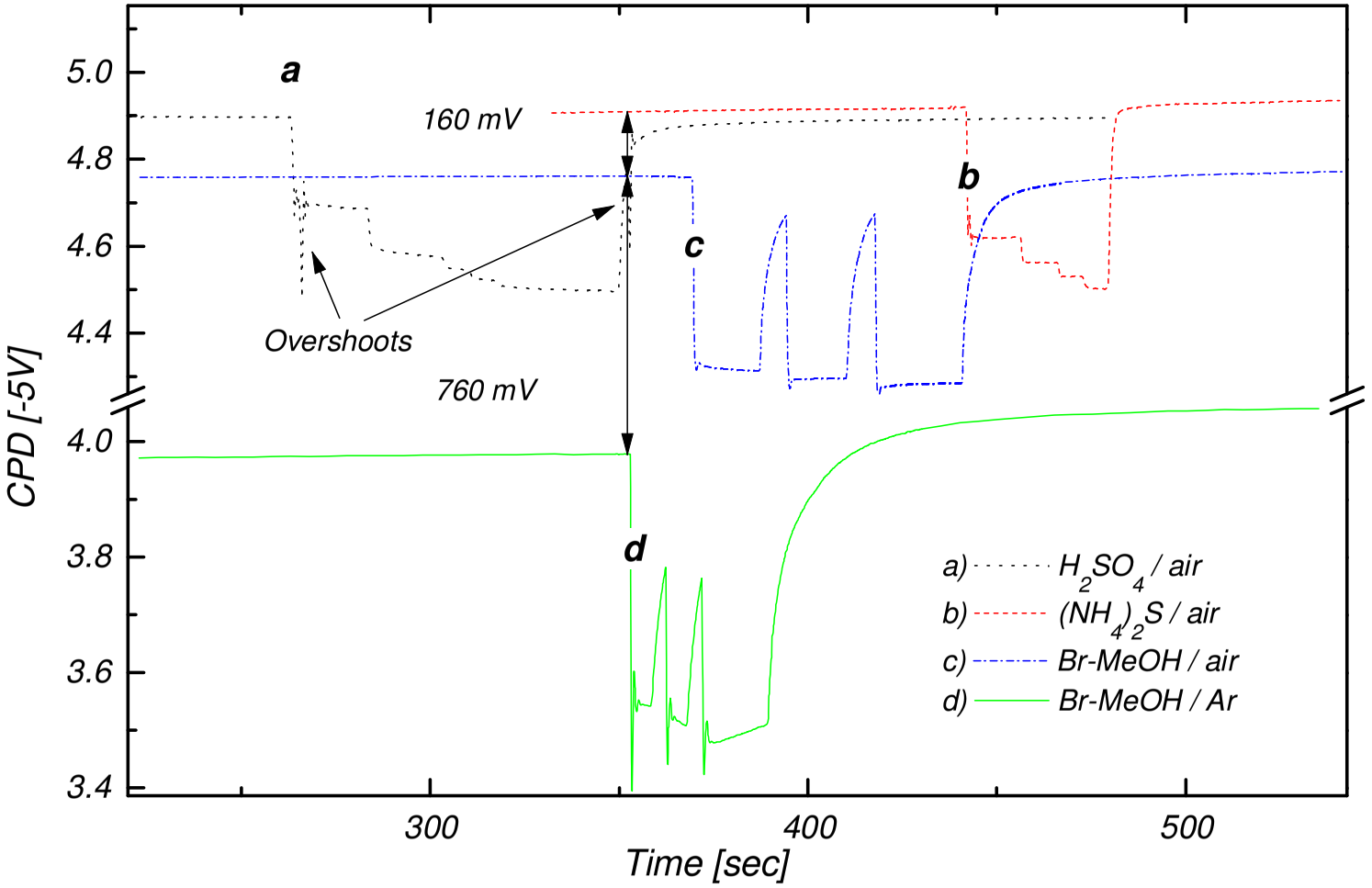

Figure 9: *Comparison between CPD values for GaAs(100) after different etching and surface treatments.*

Figure 9 demonstrates the big change introduced by the argon environment. While the net change in dark WF between three different etchings in air (9.a-c), was about 200 mV, for exactly the same etchant, in air and in Ar (9.c,d), the dark WF decrease is about 760 mV. This decrease can be an artifact or real one, i.e. it could be due to 'background' changes, like eliminating humidity influence, or ambient adsorbate on the gold probe which all modify the reference value (taken arbitrarily constant as 5V), or it may indicate a real change in sample surface like less oxide (which causes a negative dipole, hence increased electron affinity) or different reconstruction[50]. The former explanation is less likely because, while the accumulated experience with KP measurements in air shows some sensitivity to the environmental conditions, the changes are never as high as ~ 0.8 V. As most of the Kelvin probe measurement and semiconductor surface measurements in general are done in UHV, this looks like an interesting way to try to define the influence of the ambient on surface behavior.

Figure 9 shows the high sensitivity of the system to environmental contributions. Therefore the convention of reference state is problematic in regard to exact surface stoichiometry and reconstruction. It should be mentioned that all ligands were adsorbed overnight, which assured that the di-sulfides were chemisorbed to the surface, in contrast to the situation with some of the IR experiments.

3.2.2 Ligand's effect on electron affinity.

Dipole-induced changes can be measured by the change in the flat band work function, i.e. from CPD measurements under saturating illumination, because then BB effects are minimized. CPD curves for ligands adsorbed on GaAs look very much like curve 9.d. While this situation cannot be considered as flat band condition[5], it can be regarded as nearly flat band state. Even if the bands are somewhat bent at this state, the major part of the BB is flattened, and a general trend can be calculated despite the minor bending. This uncompleted flattening becomes much more of a severe problem in detecting changes in the BB itself, as can be seen in the next section.

Figure 10 shows the changes in electron affinity, as compared to the EA of a reference sample after etching and immersing in zero concentration solvent (acetonitrile), which is 3.45 ± 0.04 V. To gain insight into the ligand-substrate interaction I looked for correlation with two possible molecular properties (molecular data appears in appendix 4): the dipole of the substituted phenyl (hollow circles); and a Hammett parameter (filled circles). As shown in figure 10, the electron affinity, or surface dipole increase with positive dipole or positive Hammett parameter, since for both scales positive values represent negative surface charge.

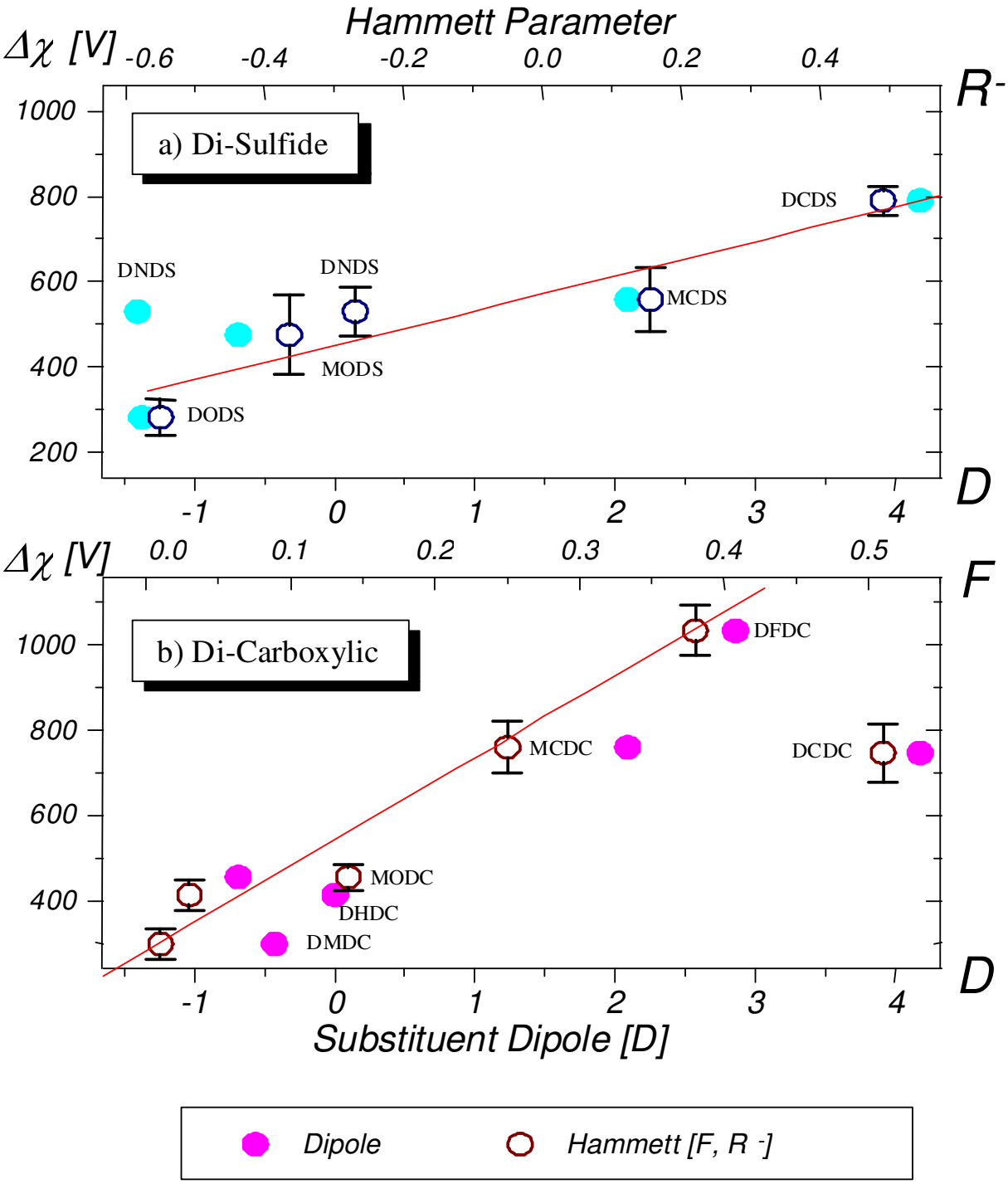

Figure 10: The effect of ligand adsorption on the electron affinity of GaAs(100).

a) Di-Sulfides; b) Di-Carboxylic.

The Hammett parameter scale places almost all the data points in monotonic order (notice DNDS and MODC). The exceptional low value of DCDC can be explained by taking into account the different surface coverage of different molecules. Coverage data for di-sulfide on gold were measured by Urs Krops[51] and are shown in appendix 5. They show that the coverage of DCDS is only 75% relative to 100% of MCDS. Especially low coverage of DCDC on GaAs can explain its low contribution to induced dipole, but no specific measurements were done. DCDS did not show an exceptionally low value.

For di-sulfides, only the negative transition state (R^- or σ^-) Hammett parameters were able to shift the DNDS data point to the right, on the figure.

The linear fit using the Hammett scale gives the following relations:

di-sulfide: $$\Delta\chi = 571 + 402 \cdot R^- \quad (3.1$$

di-carboxylic: $$\Delta\chi = 282 + 1992 \cdot F \quad (3.2$$

It should be noticed that the F and R scales are numerically different, and also their zero's do not coincide.

3.2.3 Ligands effect on band bending.

Having demonstrated ligand binding to the surface and having shown that this induces changes in surface dipoles, we expect a charge transfer between the ligand and the surface, resulting in a redistribution of surface charge. In other words, we expect the interaction to introduce new energy levels. If they differ enough from the bare surface states this should influence the surface charge, and thus the band bending. The band bending is calculated as the difference in work function between dark and light and it is always positive for n-type (bands bent upward toward the surface). Figure 11 shows the change in band bending, relative to a bare reference (BB = 626 ± 21 mV), correlated to the Hammett resonance parameter (R) for di-sulfides and to the Hammett field parameter for di-carboxylic (F). In all cases the band bending decreases as result of adsorption, with bigger changes in di-carboxylic compared to di-sulfides. The errors in BB values are much larger than in other CPD results. This is explained by the un-stable signal under illumination (see figures 9 and 12.a).

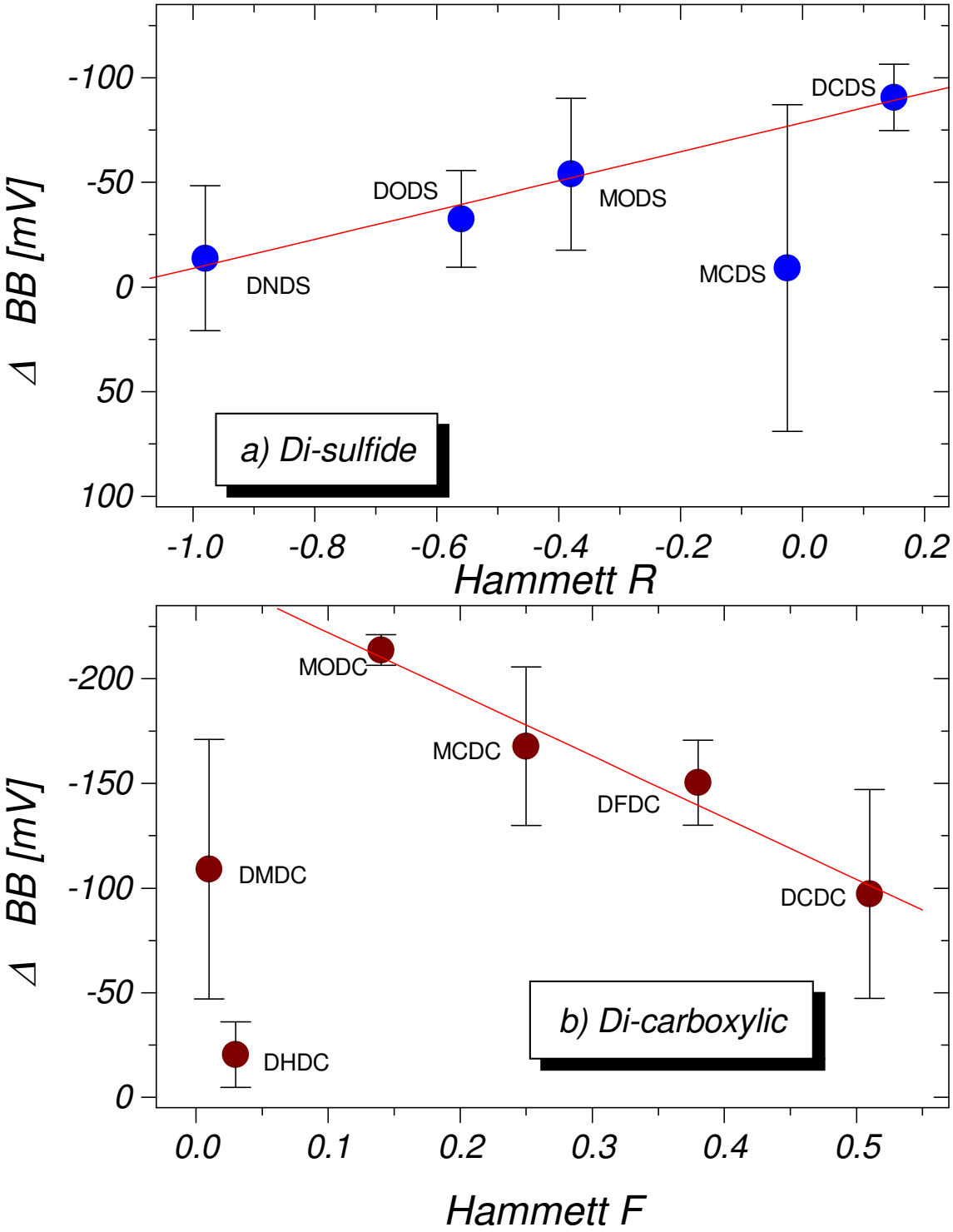

Figure 11: The effect of ligand adsorption on the band bending of GaAs(100). a) di-sulfide; b) di-carboxylic.

For the di-sulfides, the MCDS data are not reliable because of the huge error and almost zero change in BB. Excluding it, the results are well correlated to the resonance parameter (R), but could be correlated as well to positive Hammett parameters ($+\sigma_p$, +R). Di-carboxylic data can be correlated fairly well with negative parameters ($-\sigma_p$, -R), although two distinct relations exists for electron withdrawing and electron donating substituents, with MODC as turning point. It should be noticed that the BB changes could be correlated only to the Hammett parameter, and not with substituent dipole, or phenyl ionization potential (as was the case for adsorption of these ligands onto CdTe).

The linear fit discarding DHDC, DMDC, and MCDS gives the following relations:

di-sulfide: $$\Delta BB = -79 - 70 \cdot R \quad (3.3$$

di-carboxylic: $$\Delta BB = -252 + 295 \cdot F \quad (3.4$$

3.2.4 Time dependent analysis:

A different approach to extract data about charge transfer at the surface is to analyze the time-dependent behavior of the CPD. Figure 12 shows CPD evolution with time after exposing the sample to the highest light intensity (12.a) and immediately after light was turned off (12.b). The behavior of four different ligands is shown, two for each binding group, with negative (DCDC, DCDS) and positive (DMDC, DODS) dipole groups. The y axis gives the as-recorded data. i.e. CPD (not WF). The x axis is time in seconds from an arbitrarily defined t=0. Notice the very long time scale which is characteristic for the KP method.

Under illumination (fig. 12.a.) the curve starts with some 'wild overshoot' points as explained in section 3.2.1., and then more or less stabilizes. The plots end when the light is turned off, which is operator-dependent. Illumination of negative dipole ligands produced relatively stable, slightly decreasing signals. In surface charge terms it means further hole accumulation at the surface. For the positive dipoles, the opposite trend is shown, i.e. electron accumulation with proceeding illumination. DODS is a typical example for reversal of behavior under illumination (first a decrease, then an increase), which is also seen in other instances, especially for as-etched (Br) samples. Attempts to quantify the behavior under illumination failed, due to the very wide distribution of the results.

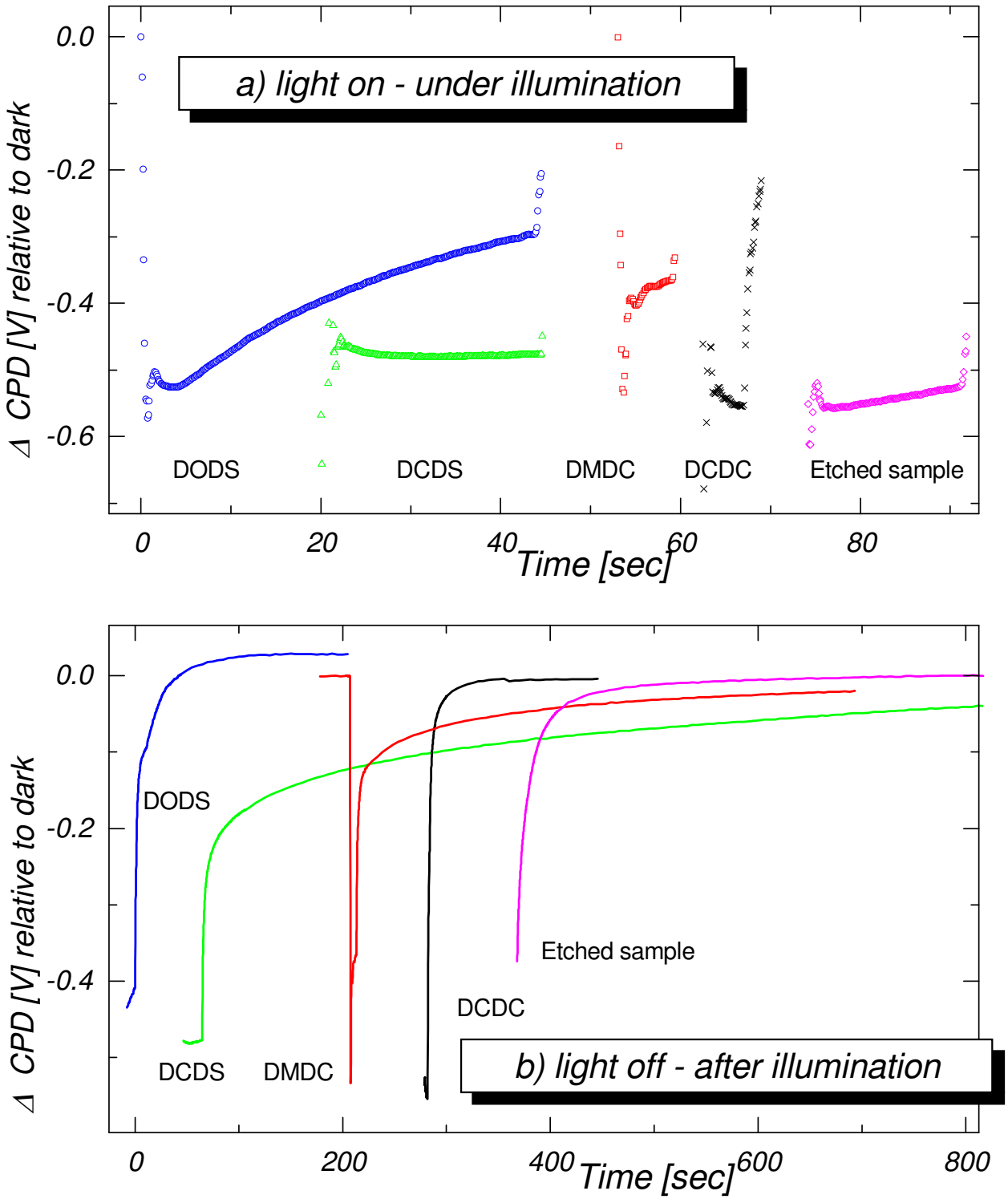

Figure 12: Evolution of CPD with time.

For clarity's sake the plots for the different ligands are displaced with respect to each other, on the time axis.

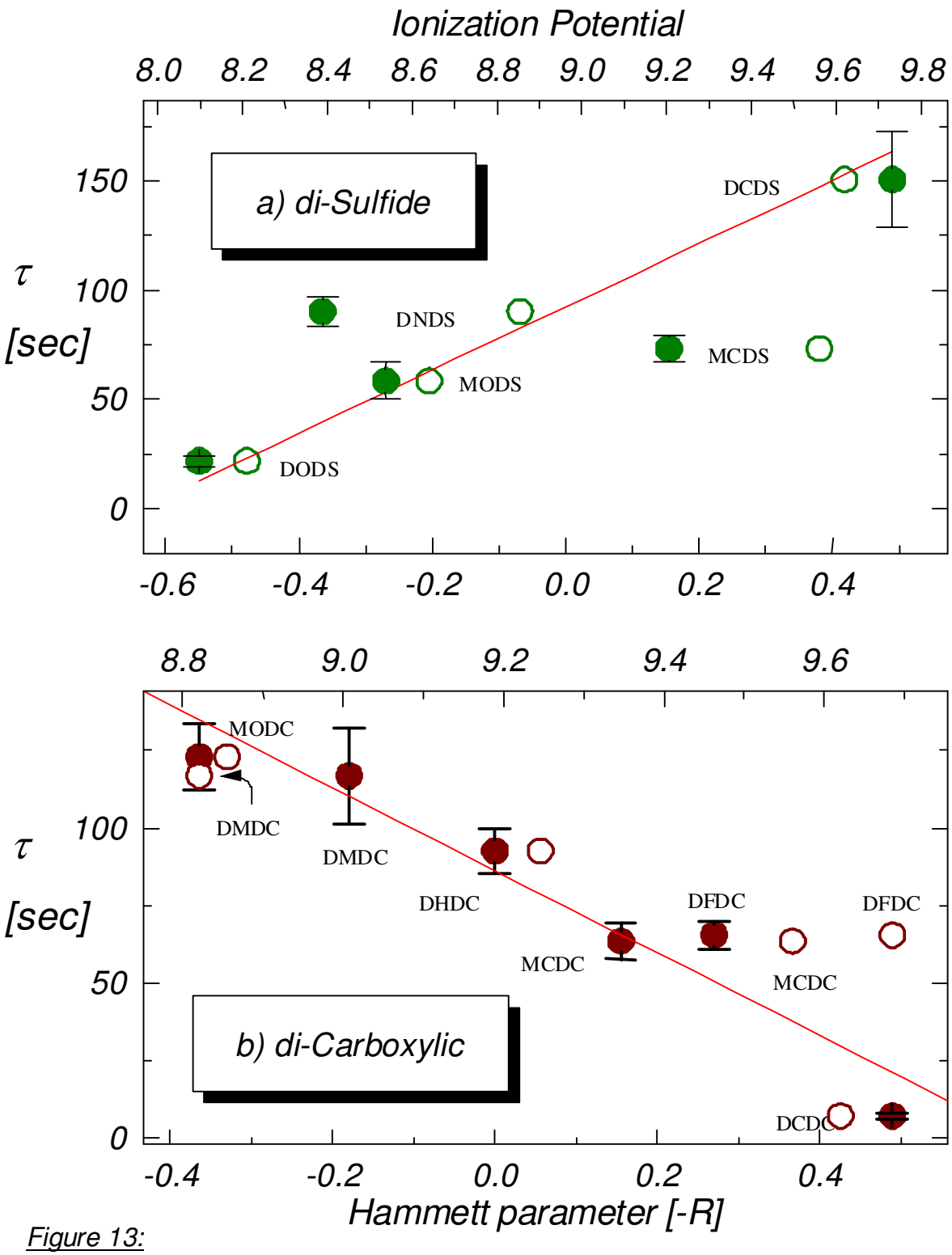

Figure 13:

The effect of ligand adsorption on the surface charge decay time.
a) di-sulfide; b) di-carboxylic

The recovery of dark equilibrium after the light is turned off, is shown in fig. 12.b. It shows both fast and slow parts. The initial fast decay is still much slower than that seen for the transition from dark to illumination and no overshoots are recorded. The whole decay cannot be fitted by a single exponential fit. However a single exponential fits to the slow part in a fairly reproducible way and is characteristic for the different ligands. The results are shown in figure 13, as decay time (τ) vs. a molecular parameter.

The striking feature in these decay times is the opposite trends for the different binding groups. This does not depend on the specific molecular property chosen for comparison, whether it is dipole moment, ionization potential or Hammett parameter. Both ionization potential (hollow marks) and Hammett parameter (filled marks) gave reasonable correlation. The negative resonance (R^-) was the type of Hammett parameter which fit the best for both di-sulfide and di-carboxylic ligands.

The linear fit with IP for di-sulfide (discarding MCDS) and with R^- for di-carboxylic gives the following relations:

di-sulfide: $$\Delta\tau = -732 + 92 \cdot \mathrm{IP} \qquad (3.5$$

di-carboxylic: $$\Delta\tau = 86 - 133 \cdot \mathrm{R}^- \qquad (3.6$$

The decay time for etched samples was much less reproducible, and few characteristics times were found. Half the samples have slow decay of 201 ± 56 sec and half the samples have much faster decay of only 31 ± 10 seconds.

Summary of KP results:

Adsorption of di-sulfide and di-carboxylic ligands on GaAs (100) induces significant changes in electron affinity and in the rate of decay of the surface charge, and somewhat smaller changes in BB. These changes can be correlated well with different molecular properties. In the following discussion section, I will try to interpret these observation in terms of a binding mechanism.

4. Discussion:

4.1. Chemistry of the binding

4.1.1 Adsorption strength:

Langmuir isotherms showed that the di-carboxylic ligands bind much faster to the surface than di-sulfides. For the di-carboxylic binding group, the substituent changes the binding constants by up to one order of magnitude between DCDC and DHDC. This difference may be reflected also in the change in BB, upon ligand adsorption, which is nearly zero for DHDC and ~100 mV for DCDC. The calculated binding energy is ~37 kJ/mol and is much higher than the binding energy of benzoic acids (see table 2). This increment is explained mainly by two binding sites compared to the single site in the benzoic acids.

The measured isotherm for di-sulfide probably represents physisorption, and the binding energy is considerably lower, as expected. A reliable isotherm for chemisorbed di-sulfide is important to compare to the di-carboxylic binding. In continuing this work, measurement of the binding constants to other substrates may give significant information, as can be seen for benzoic acids (table 2), where the binding strength increased with decreasing ionicity of the substrate[24].

4.1.2 Adsorption type:

The IR results show clearly that di-carboxylic ligands adsorb to the surface as carboxylates. The following types of carboxylate to metal binding are generally distinguished: unidentate, bidentate and bridging. They are identified by the separation ($\Delta\nu$) between the asymmetric and the symmetric carboxylate bands. For unidentate binding $\Delta\nu$>200 cm^{-1}, for bidentate $\Delta\nu$<100 cm^{-1}, and for bridging 100 < $\Delta\nu$ < 200 cm^{-1}[52]. It is possible to assign the 1644 and 1330 cm^{-1} bands to a unidentate mode, and the 1550 and ~1400 cm^{-1} (fig. 5.a,b) to a bridging form. The results show that it is unlikely that there is any bidentate complex.

There is no direct evidence to tell to which surface element the carboxylate binds. However, chemically it is reasonable to assume that it binds to the more electropositive Ga atoms. The IR spectrum of Ga benzoate showed exactly the same peaks as those of adsorbed benzoic acids on GaAs (100)[24]. The two different binding forms may be due to molecular restrictions or due to different surface sites, e.g. binding to Ga is in the more ionic form of unidentate, and to As in the more polarizable form of bridging. Different surface sites can be more

complicated than simply different elements, due to surface oxides, defects or atoms of the same element but on different reconstruction sites. The mixed binding types agree with the two site Langmuir isotherm found for di-carboxylic ligands, although those sites can be identical ones, as well.

4.1.3 Hard and soft binding:

Indirect information on the binding can be gotten from their influence on the electronic properties[11]. For both changes in EA and BB, the effective parameter for DC was the field effect (F) Hammett parameter, while for DS the resonance (R) parameter dominates (fig. 10, 11). This suggest that DC are more 'hard' and localized, while DS are more 'soft' and polarizable, and the high polarizability is expressed by the fit to the resonance parameter. The polarizable nature of organic sulfides was also found by others, who conclude that they bind to more polarizable surface sites such as As[11]. In the same manner it can be assumed that DC binds to localized electronic sites such as Ga.

The different field / resonance characteristics can also be used to explain the fact that DC are much more effective in changing the EA than DS. This is seen from the slope of change in EA per dipole moment which is almost two times larger for the DC than for the DS (fig. 10).

4.1.4 The substrate surface:

Any attempt to understand the adsorption chemistry must regard the specific pre-adsorption surface composition. The results suggest that working under Ar produces a nearly oxide-free surface. Indication for this comes from the very large reduction in WF for etched surfaces in Ar (fig. 9.d), which fits with removing the negative charge of the oxides. The CPD signal of etched GaAs under Ar is highly perturbed (not shown in the results). This suggest there is no stabilizing oxide layer, and the ligand adsorption acts to stabilize the surface in a manner somewhat similar to oxidation. Adsorption makes the surface more reproducible, although it does not eliminate surface states to give passivation as inorganic sulfur treatments[14]. Measurements done in air, with the same ligands and substrate resulted in substantially different BB[53]. This further supports the assumption that no oxide is involved when adsorption is done under Ar.

4.2. New features due to adsorption

4.2.1 Change in polarizability:

The theoretical change in EA, calculated according to equation 1.3 [4], gives $\Delta EA = 2.13$ V (see app. 3), while the experimental value is only 0.7 V (fig. 10). A number of reasons can explain this discrepancy. Firstly, the polarizability was taken for the organic part ($\alpha \approx 34 \cdot 10^{-24}$ cm^3), while organo-metallic complexes have much higher polarizabilities ($\alpha \approx 60 \cdot 10^{-24}$ cm^3, see app. 4, table 5). Secondly, we did not consider the molecular tilt (θ) which reduces the effective dipole by $\cos(\theta)$. The tilt of DS adsorbed on gold was $\theta \approx$ 50-55° [26] . Calculating the expected change in electron affinity with these two corrections gives: $\Delta EA = 0.9 \sim 1$ V, which is much closer to the experimental value.

Another approach to calculate the induced field replaces the polarizability of the isolated molecule (α) by an average permittivity of the film (ε), which, in special cases, can be determined experimentally[54] or can be taken as a fitting parameter. Using this approach the experimental ΔEA value can be calculated with $\varepsilon \approx 6.7$ - 4.33 with 0° or 50° tilt respectively. These values are reasonable compared to experimental permittivities of similar molecules reported in the literature[54]. Using permittivity instead of single molecule polarizability suggests that the behaviour that we are looking at cannot be related solely to a property of the isolated molecule, but reflects also a collective molecular property. This approach is used to explain observations presented in following sections (4.2.2, 4.2.3).

4.2.2 Change in intrinsic dipole moment:

All ligands increase the EA regardless of binding group or substituent. Both DS and DC ligands with a substituent dipole around 0, increased the EA by ~0.5 V (fig. 10). For comparison, benzoic acids, with no intrinsic dipole, have no influence on the EA[24]. The constant dipole contribution can be explained by a strong negative dipole on the 'skeleton' of the ligand, and / or on the bond itself[26]. The former is related to the charge distribution inside the molecule, while the latter refers to charge distribution between the substrate and the molecule.

Regarding the first assumption, we can estimate from figure 10 the magnitude of the additional dipole required to eliminate the change in EA. It is about 5.7 D for DS and 4.1 D for DC. The dipole (p) that is induced due to the bond itself (second assumption) depends on the percent ionic character (I) of the bond: $p = I \cdot q \cdot r$, where q is the electronic charge and r is the bond length. The percent of ionicity, I, is calculated by using Pauling electronegativities[55], and detailed calculations appear in app. 3.

They show that the oxygen - Ga bond can have a bond-induced dipole up to -2.4 D (for p orbital), while the sulfur (in sp^2 hybridization) can induce a bond dipole of -1.3 or -2.6 D if it binds to As or Ga, respectively (see app. 3, table 3). The 'skeleton' contribution to the dipole can be estimated from DS adsorption on Au and $CuInSe_2$, where it was found to be ~ -1.5 D[26]. If we add this value to the bond-induced dipole we reach the experimental shift in dipole moment for DC, and somewhat less for DS (especially if we assume that S binds to As). In the case of benzoic acid adsorbed on GaAs changes in electron affinity were directly related to the molecular dipole of benzoic acid[24] without any shift. This is so, not withstanding despite the fact that the bound form of the ligand is carboxylate. Therefore it can be said that in this case the dipole of XPhCOO - **H** is very similar to that of XPhCOO - **Ga** and that this dipole includes both the molecule 'skeleton' and the surface bond contributions.

The direction of the additional dipole is negative (increase in EA) which fits the higher electronegativity of O or S relative to Ga or As. This indicates that both types of ligands are acidic in character, which agrees with the direction of change in BB (fig. 11), where ligands act to reduce the surface charge. Yet it is not obvious that one can view the carboxylate as an acid. It may suggest that it is the carboxylic acid that binds, rather than the carboxylate.

Another possible explanation for the increase in EA at 0 surface dipole, can be obtained by considering the large decrease in work function for the etched sample in Ar relative to air (~ 0.6 V, fig. 9.c,d), or relative to literature values (~-0.4V, app. 6)[50]. Chen et. al.[50] showed that different reconstruction can influence the EA up to 0.4 eV. Our very low initial EA value indicates a Ga rich surface, and it may suggest that the ligands alter the surface reconstruction, by removing excess Ga or simply by breaking the dimerization. This process can account for the whole shift in EA.

4.2.3 Di-sulfide resonance dependence:

The strong dependence of the change in BB of DS on the Hammett resonance parameter is unexpected, because there is no conjugation inside the molecule between the phenyl part and the di-thiane ring. Nevertheless, the arranged array of molecules on the surface probably results in a new entity with properties somewhat different from those of a single isolated molecule. Also the IR results of the chemisorbed DS layer (fig. 5.C) suggest some kind of intra-layer interactions between the carbonyl groups. Therefore it seems that adsorbed ligand interactions with the surface can not always be explained only by isolated properties, and collective properties can contribute significantly.

4.3. Ligand interactions with the surface

4.3.1 Electron transfer processes:

The slow decay is very sluggish for electronic processes, as noted in the literature before [7,6, 5]. In physical terms, there is a barrier for equilibrium between the delocalized bulk states and the localized surface states[5]. This barrier can be viewed as electron transfer from one isolated state to another, but can not be explained by de-excitation from one energy level to another which is much faster. Charge trapping is not originated by the ligands, since it exists also in clean surfaces. However, the results show that the adsorbed ligands interact with the traps and either shift their energy level closer to band edges, or either they produce an alternative route for releasing the trapped charge.

4.3.2 Correlation between ΔBB and Hammett parameters (fig. 11):

Correlating the changes in BB with Hammett parameters reveals interesting features. The ΔBB of DC can be correlated with the field effect (F) parameter or with negatively charged transition states, while DS correlates better with resonance effect (R) or positively charged transition states. The F and R behavior is explained above (sec. 4.1.3). The correlation with transition states suggests that the molecule (or part of it, because the Hammett parameter is taken only for the substituent) behaves like an unstable charged particle. The correlation of DC with a negative transition state, suggests that the new energy levels of the adsorbed ligands are comparable to excess of electrons on the ligand. It suggests that DC ligands withdraw electrons from the surface to their LUMO. In the same way, the correlation of DS with positive transition states suggests that they donate electrons from their HOMO. This picture (mainly for DS) contradicts the negative dipole which both ligands showed, i.e. electron distribution is toward the ligands. At this moment we do not have a clear picture of how the transition state, which is a reaction coordinate concept, is expressed in the effect of ligand adsorption on the band bending (see, however, section 4.3.4 below).

In air the influence of molecules on the BB is opposite to the above results (in argon) as measured by KP[53] and by MOCSER [29]. There, adsorption of DCDC increases the BB by about 200 mV, i.e. increases the surface charge, and also in absolute values the BB was much higher in air than in Ar. This can be related to the question of oxidation of the carboxylic acid to carboxylate, and to where goes the proton. This mechanism may

be different in air (with minor quantities of oxide on the surface) and under Ar, and can totally change the role of DC from acidic in Ar (decrease BB) to basic in air (increase BB).

4.3.3 CPD changes in terms of charge accumulation:

Tracing the change of CPD in time (figs. 9 and 12) shows decreases and increases i.e. positive and negative charge accumulation at the surface, respectively. The sharp decrease under illumination (fig. 9) is the band flattening due to accumulation of photoinduced holes (minority carriers) at the surface. Further illumination can cause a slow change in surface potential up to 150 mV (fig. 12.a). For the case of DODS the illumination excites (electronically) holes very fast, but later they decay (chemically) from the surface, probably by transfer to the isolated energy levels of the ligands. This process is clearly controlled by the specific molecular properties, and differs from one substituent to another.

For all ligands, turning the light off is accompanied by positive charge trapped at the surface, as can be seen from the shape of the decay curves in figure 12.b. For the opposite case, of trapping a negative charge, the CPD would immediately 'jump' above its original value because trapped electrons act to increase the surface potential, which is the same trend as the influence of turning off the light (electronic rapid decay of photoinduced holes).

4.3.4 Direction of the slope in Hammett correlation for ΔBB and decay rate:

Although the trapped charge is of the same sign for both types of ligands (fig. 12), the dependence on molecular properties is opposite (fig. 13), with the DS decay faster with electron donating groups, and the DC decay faster with electron withdrawing substituents. The opposite slopes can also be seen for the correlation of molecular properties with ΔBB (fig. 11). In general it can be said that ligands with large influence on the BB are the slowest to release the trapped charge. However in both cases adsorption of ligands reduces the surface charge (decrease the band bending) and traps holes under illumination.

This seeming discrepancy can be explained using the Hammett convention: $\log\left(\frac{k}{k_o}\right) = \sigma \cdot \rho$, where k_o is the rate constant or equilibrium constant for X=H, k is the constant for any other group X, ρ is a constant for a given reaction under a given set of conditions, and σ is a constant characteristic of the group. For $\rho > 0$ the reaction is facilitated by electron removal from the reaction zone; for $\rho < 0$ the reaction is retarded by electron

removal. The Hammett equation has also been shown to apply to many physical measurements, including IR frequencies and NMR chemical shifts[56, 57].

In order to interpret the correlation with Hammett parameter we must specify the involved reaction. The electronic measurements (CPD) do not relate to the adsorption mechanism, however we suggest that the amount of ΔBB can be related to the degree of interaction between the ligand orbital and the surface states, and that the decay rate can be viewed as a chemical process of electron transfer between the adsorbate and the bulk bands (without desorption of the ligand)[3]. The exact formulation of these process is still unclear, as discussed in the next section.

4.4 Suggested interpretation for chemical-electronic process:

In this final section I will try to relate the above observations to common concepts of surface chemistry and physics. A schematic model is presented in figure 14. The main observations (underlined) and conclusions drawn from them, were:

- Both DC and DS decrease the BB, therefore adsorption shifts the energy levels out of the forbidden gap, by lowering deep states below the valence band maximum and / or raising the higher states above the Fermi level.
- From the opposite trends observed in ΔBB between DS and DC (4.3.3), we conclude that among DS, cyano (DCDS) has the strongest interaction with the surface states, and therefore has the largest energy level separation of the bonding and anti bonding orbitals of the adsorbate - surface complex. With DC the situation is opposite, and methoxy has the strongest surface interaction, resulting in the largest separation. The exact nature of interaction, whether the HOMO or the LUMO of the ligand interact, with filled or empty surface states is unclear at the moment.

- From the energetic point of view the results may be explained by taking the DS energy position above that of the relevant surface states (fig. 14.a.), and therefore the electron withdrawing substituent (e.g. cyano) *lowers* the energy of the ligand *closer* to the level of the surface states. Taking the DC energy level below that of the relevant surface states, causes higher energy substituents (e.g. methoxy) to bring the ligand's level closer to the surface state levels and thus to increase their interaction. This theory is supported by comparing the estimated LUMO of the ligand (i.e. EA) with energy levels of the surface (fig. 14.b; EA was calculated by Rami Cohen[34]). It shows that as the LUMO is closer in energy to the mid-gap states it has the strongest influence on the BB.

- At the moment ligand energy levels for DS can not be estimated. However, the view of high energy DS and low energy DC (fig. 14.a.) is supported by the ionization potentials of molecules similar to di-thiane (IP ≈ 8.2 eV) and tartaric acid (IP ≈ 9.8 eV) (see appendix 4, table 5). Even though these values are much below the work function of GaAs (fig. 14.b.), they indicate the trend of higher energy position of DS relative to DC (the problem of too low energy levels can be addressed by assuming the ligands interact via their LUMO and not by the HOMO).

- The seemingly un-ordered plot in fig. 14.b. is due to the use of an energy scale. As shown in the results (fig. 11.b.), using the Hammett field parameter yields an ordered ΔBB dependence. As mentioned in the introduction (1.3) orbital overlap and the nature of the transition state can be as important as the energetics in determining the extent of interactions between molecular orbitals and solid bands[3]. Correlation with Hammett parameters is one possibility to account for considerations other than energetic ones. Other important contributions for stabilization / destabilization of the adsorbed complex, such as the solvent effect, are not considered here simply because we do not have at the moment the means to estimate them.

- An explanation, similar to that presented above for the opposite effect of substituents, can be given using hard / soft acid / base interactions. The polarizability of 'soft' DS will increase by electron withdrawing substituents (cyano) while the localization (or ionicity) of DC is increased by electron donating groups (methoxy).

- The slope of ΔBB vs. Hammett parameters (ρ) is positive for DS and negative for DC. According to Hammett theory (4.3.4), DS - surface interaction is facilitated by electron removal from the reaction zone, and DC interaction by electron addition. This agrees with positive and negatively charged "transition states" found for DS and DC, respectively.
- The correlation of ΔBB with the DS Hammett parameter can be interpreted in terms of a positively charged transition state by assuming that the bonding states of the new complex are more 'surface-like', and that the bonding electrons are localized closer to the surface, leaving the ligand with a slight positive charge. Positive charge on DS can be also be explained by interaction with empty surface states that withdraw electrons from the ligand. The correlation of ΔBB with the DC Hammett parameter can be interpreted in terms of a negatively charged transition state, if the carboxylate (anionic) mode revealed by FTIR is taken to indicate the nature of that state. It agrees with an energy position of the free ligand below the surface state level, allowing withdrawal of electrons from the surface to the ligand.

Unanswered questions:

- Large changes in ΔBB were accompanied by slow decay of surface traps. The question is whether large ΔBB & slow decay represent strong interaction with the surface, or if it is the opposite case. Intuitively, fast decay means shallow traps, i.e. closer to the band edges, while small BB (large ΔBB) requires shifts of the surface states out of the energy gap or above the Fermi level. These requirements contradict each other. Significant information regarding the interaction strength can come from adsorption isotherms for different substituents, planed to be done. The two ligands already measured (DCDC & DHDC) do show a positive relation between ΔBB and K (4.1.1).
- The effect of adsorption on the trapping mechanism is still unclear. Deep traps in GaAs are well-known from the literature for clean surfaces (under UHV)[4,5,6], with characteristic times similar to those observed here. In our experiments all ligands reduce the decay time relative to the etched sample. Therefore, ligands influence the trapping mechanism, but do not originate it.
- The basic or acidic character of the ligands is not clearly verified. Most experimental evidence suggests that the ligands are acidic toward the surface (increased EA, reduced BB), but the chemistry of the bound ligands (COO^-) and the opposite effects of the substituents on the ΔBB of DC and DS ligands are difficult to settle.

5. Summary:

In continuation to extensive work on binding of organic ligands done in this group and by others, I succeeded to bind tailor-made ligands to the surface of GaAs. Despite the highly un-stable surface of GaAs, adsorption could be done at ambient pressure, though mostly inert argon atmosphere was used. The use of GaAs as a substrate is meaningful if one considers future utilization of ligands in electronic devices.

Infrared spectroscopy reveals di-carboxylic ligands to form a carboxylate complex with the surface. Binding to the semiconductor was by unidentate and bridging forms, and also the isotherms follow a double site binding mechanism. The resulting layers have high stability toward rinsing, and only a polar solvent, such as methanol was able to remove the layer. The adsorption constant (37 kJ/mol for DCDC), evaluated by fitting to a Langmuir isotherm, is fairly high, relative to reported binding constants of organic ligands to semiconductor surfaces.

Significant changes in surface physical properties were induced by the adsorption. The electron affinity increased up to 1 V relative to 3.45 for a bare GaAs surface. Ligand adsorption was able to unpin the GaAs surface up to 200 mV, relative to original band bending of 600 mV. However the ligands were not able to totally remove the surface charge, or passivate the surface as efficiently as inorganic surface treatments. Adsorption alters the deep surface traps, as can be seen by the reduced decay time of the CPD from the illuminated quasi-equilibrium to dark equilibrium. Ligands were able to reduce the decay time from ~200 sec down to ~10 sec.

Correlation of the changes in CPD with various molecular parameters revealed additional insight into the chemical nature of the interactions. It was found that both ligands act as acids toward the surface (since the BB is reduced) but DC has hard ionic interactions, while DS has soft polarizable interactions. Despite the fact that all ligands increase the electron affinity, the bonding electrons are closer to the surface in DS adsorption, and closer to the ligand in DC adsorption, as revealed by the correlation of ΔBB to positive and negatively charged transition states, respectively. Interpretation of the results suggests that collective molecular phenomena arise by the adsorption, and parameters of isolated molecules can not explain the whole picture.

This study raises many question regarding the interactions of ligands with semiconductor surfaces. At the moment we have only partial answers. However they indicate that intelligent use of molecular parameters, considering both the binding group and the remote group can yield pre-determined control of the surface properties of GaAs, as well as of other semiconductors.

6. References:

1. M. C. Petty, M. R. Bryce, and A. Bloor, *An Introduction to molecular electronics*, Edward Arnold, London, 1995.
2. M. Grn̈tzel, "The artificial leaf, molecular photovoltaics achieve efficient generation of electricity from sunlight",*Coordination Chemistry reviews*, **111**, 167 (1991).
3. R. J. D. Miller, G. L. McLendon, A. J. Nozik, W. Schmickler, and F. Willig, *Surface Electron Transfer Processes*, VCH publishers, New York, 1995.
4. W. Mɤnch, *Semiconductor Surfaces and Interfaces*, Springer, Berlin, 1995.
5. B. I. Bednyi, M. I. Vasilevsky, and I. A. Karpovitch, "Determination of the surface band bending from the kinetics of a barrier -trap photo emf",*Sov. Phys. Semicond.*, **23**, 223 (1989).
6. K. Stiles, D. Mao, and A. Kahn, "Oxygen adsorbed on GaAs(110) surfaces: The effect of temperature on band bending",*J. Vac. Sci. Technol. B*, **6**, 1170 (1988).
7. T. U. Kampen, D. Troost, X. Y. Hou, L. Koenders, and W. Mɤnch, "Surface-photovoltage effects on adsorbate-covered semiconductor surfaces at low temperatures",*J. Vac. Sci. Technol.*, **B9**, 2095 (1991).
8. P. C. Stair, "The Concept of Lewis Acids and Bases Applied to Surfaces", *J.Am.Chem.Soc.*, **104**, 4044 (1982).
9. T. Wolkenstein, *Electronic Processes on Semiconductor Surfaces during Chemisorption*, Consultants Bureau-Plenum Publishing Corporation, New York, 1991.
10. K. D. Kepler, G. C. Lisensky, M.Patel, L. A. Sigworth, and A. B. Ellis, "Surface-bound carbonyl compounds as Lewis acids. Photoluminescence as a probe for the binding of Ketones and Aldehydes to Cadmium Sulfide and Cadmium Selenide surfaces.",*Journal of Physical Chemistry*, **99**, 16011 (1995).
11. S. R. Lunt, P. G. Santangelo, and N. S. Lewis, "Passivation of GaAs surface recombination with organic thiols",*J. Vac. Sci. Technol. B*, **9**, 2333 (1991).
12. C. J. Sandroff, M. S. Hedge, and C. C. Chang, "Structure and stability of passivating arsenic sulfide phases on GaAs surfaces",*J. Vac. Sci. Technol.*, **B7**, 841 (1989).

13. C. J. Sandroff, R. N. Nottenburg, J.-C. Bischoff, and R. Bhat, "Dramatic enhancement in the gain of a GaAs/AlGaAs heterostructure bipolar transistor by surface chemical passivation",*Appl. Phys. Lett.*, **51**, 33 (1987).
14. B. A. Cowans, Z. Dardas, W. M. Delgass, M. S. Carpenter, and M. R. Melloch, "X-ray photoelectron spectroscopy of ammonium sulfide treated GaAs(100) surfaces",*Appl. Phys. Lett.*, **54**, 365 (1989).
15. J. Yota and V. A. Burrows, "Chemical and electrochemical treatments of GaAs with Na_2S and $(NH_4)_2S$ solutions: A surface chemical study.",*J. Vac. Sci. Technol. A*, **11**, 1083 (1993).
16. M. G. Nooney, V. Liberman, and R. M. Martin, "Sulfur layer formation on GaAs(100) by thermal and photochemical H_2S dissociation",*J. Vac. Sci. Technol. A*, **13**, 1837 (1995).
17. J. Yota and V. A. Burrows, "Surface chemistry of GaAs treated with buffered HF and NH4F solutions: Slow reactions of process residuals",*J. Vac. Sci. Technol. A*, **10**, 837 (1992).
18. J. A. Dagata, W. Tseng, J. Bennett, J. Schneir, and H. H. Harary, "P_2S_5 passivation of GaAs surfaces for scanning tunneling microscopy in air",*Appl. Phys. Lett.*, **59**, 3288 (1991).
19. A. N. MacInnes, M. B. Power, A. R. Barron, P. P. Jenkins, and A. F. Hepp, "Enhancement of photoluminescence intensity of GaAs with cubic GaS chemical vapor deposited using structurally designed single-source precursor",*Appl. Phys. Lett.*, **62**, 711 (1993).
20. C. W. Sheen, J.-X. Shi, J. Martensson, A. N. Parikh, and D. L. Allara, "A new class of organized self-assembled monolayers: alkane thiols on GaAs (100)",*J. Am. Chem.*, **114**, 1514 (1992).
21. K. Asai, T. Miyashita, K. Ishigure, and S. Fukatsu, "An application of electrolytic deposition for electronic passivation of GaAs surfaces through the formation of thin organic films",*Surface Science*, **306**, 37 (1994).
22. O.S.Nakagawa, S. Ashok, C. W. Sheen, J. Martensson, and D. L. Allara, "GaAs Interfaces with Octadecyl Thiol Self-Assembled Monolayer: Structural and Electrical Properties",*Japanese Journal of Applied Physics*, **30**, 3579 (1991).
23. S. R. Lunt, G. N. Ryba, P. G. Santangelo, and N. S. Lewis, "Chemical studies of the passivation of GaAs surface recombination using sulfides and thiols",*J. Appl. Phys.*, **70**, 7449 (1991).
24. S. Bastide, R. Butruille, D. Cahen, A. Dutta, J. Libman, A. Shanzer, L. Sun, and A. Vilan, "Controlling the work function of GaAs by chemisorption of benzoic acid derivatives", submitted to *J. Phys. Chem.*, (1996).

25. M. Bruening, E. Moons, D. Yaron-Marcovich, D. Cahen, J. Libman, and A. Shanzer, "Polar Ligand Adsorption Controls Semiconductor Surface Potentials",*J. Am. Chem. Soc.*, **116**, 2972 (1994).
26. M. Bruening, R. Cohen, J. F. Guillemoles, T. Moav, J. Libman, A. Shanzer, and D. Cahen, "Simultaneous Control of Surface Potential and Wetting of Solids with Chemisorbed Multifunctional Ligands",submitted to *J. Amer. Chem. Soc.,* (1996).
27. R. Cohen, S. Bastide, D. Cahen, J. Libman, A. Shanzer, and Y. Rosenwaks, "Controlling Band Bending and Electron Affinity of CdTe by Adsorption of Dicarboxylic Acids",*submitted to Advanced Materials* (1996).
28. D. Gal, E. Sone, R. Cohen, G. Hodes, J. Libman, A. Shanzer, H. W. Schock, and D. Cahen, "Engineering the Interface Energetics of Solar Cells by Grafting Molecular Properties onto Semiconductors",*Submited* (1996).
29. K. Gartsman, D. Cahen, A. Kadyshevitch, J. Libman, T. Moav, R. Naaman, A. Shanzer, V. Umansky, and A. Vilan, "Molecular control of GaAs transistor",*Submitted to Phys. Rev. Lett.* (1996).
30. D. Lin-Vien, N. B. Colthup, W. G. Fateley, and J. G. Grasselli, *The handbook of infrared and Raman characteristic frequencies of organic molecules*, Academic Press, San Diego, 1991.
31. S. H. Chen and C. W. Frank, "Infrared and fluorescence spectroscopic studies of self-assembled n-alkanoic acid monolyers",*Langmuir*, **5**, 978 (1989).
32. R. J. Jakobson, *Fourier transform infrared spectroscopy. Applications to chemical systems*, J. R. Ferroro and L. J. Basile, Eds., Academic Press, New York, 1979.
33. D. L. Allara and R. G. Nuzzo, "Spontaneously Organized Molecular Assemblies. 2. Quantitative Infrared spectroscopic determination of equilibrium structures of solution-adsorbed n-alkanoic acids on an oxidized aluminum surface",*Langmuir*, **1**, 52 (1985).
34. R. Cohen, personal communication, WIS, 1996.
35. S. Trakhtenberg, personal communication, WIS, 1996.
36. N. A. Surplice and R. J. D'Archy, "A critique of the Kelvin method measuring work functions",*J. Phys. E: Sc. Instr.*, **3**, 477 (1970).
37. W. A. Zisman, "A new method of measuring contact potential differences in metals",*R.S.I.*, **3**, 366 (1932).

38. L. Kronik, L. Burstein, Y. Shapira, and M. Oron, "Laser surface photovoltage spectroscopy: a new tool for the determination of surface state distributions",*Appl. Phys. Lett.*, **63**, 60 (1993).
39. A. K. Henning, T. Hochwitz, J. Slinkman, J. Never, S. Hoffmann, P. Kaszuba, and C. Daghlian, "Two-dimensional surface dopant profiling in silicon using scanning Kelvin probe microscopy",*J. Appl. Phys.*, **77**, 1888 (1995).
40. B. H. Blott and T. J. Lee, "A two frequency vibrating capacitor method for contact potential difference measurement",*Journal of Scientific Instruments (Journal of Physics E)*, **2**, 785 (1969).
41. K. Besocke and S. Berger, "Piezoelectric driven Kelvin probe for contact potential diffrence studies",*Rev. Sci. Instrum.*, **47**, 840 (1976).
42. F. Rossi, "Contact Potential Measurement: Spacing-Dependence Errors",*Rev. Sci. Instrum.*, **63**, 4174 (1992).
43. I. D. Baikie, E. Venderbosch, J. A. Meyer, and P. J. Z. Estrup, "Analysis of stray capacitance in the Kelvin method",*Rev. Sci. Instrum.*, **62**, 725 (1991).
44. B. Ritty, F. Wachtel, R. Manquenouille, F. Ott, and J. B. Donnet, "Conditions necessary to get meaningful measurements from the Kelvin method",*J. Phys. E.*, **15**, 310 (1982).
45. M. Bruening, E. Moons, D. Cahen, and A. Shanzer, "Controlling the Work Function of CdSe by Chemisorption of Benzoic Acid Derivatives and Chemical Etching",*Journal of Physical Chemistry*, **99**, 8368 (1995).
46. C. J. Pouchert, “The Aldrich Library of FT-IR Spectra”, Aldrich Chemical Company, Milwaukee, 1985.
47. S. D. Mukherjee and D. W. Woodard, *Gallium Arsenide*, M. J. Howes and D. V. Morgan, Eds., John Wiley & Sons Ltd, 1985.
48. M. Bruening, “Controlling semiconductor and metal surfaces via organic ligand adsorption”, *Ph.D. thesis*, Weizmann Institute of Science, Rehovot, 1995.
49. D. Yaron-Marcovich, “Studies of the adsorptioin mechanism of polar ligands on the surface of chalcogenide semiconductors”, *M.Sc. thesis*, Materials and Interfaces, Weizmann Institute of Science, Rehovot, 1994.
50. W. Chen, M. Dumas, D. Mao, and A. Kahn, "Work function, electron affinity, and band bending at decapped GaAs(100) surfaces",*J. Vac. Sci. Technol. B*, **10**, 1886 (1992).
51. U. Krops, personal communication, WIS, 1996.

52. K. Nakamoto, *Infrared and Raman Spectra of Inorganic and Coordination Compounds*, John Wiley & Sons, New York, 1986.
53. R. Davids, unpublished results, WIS, 1996.
54. O. N. Oliveira, D. M. Taylor, T. J. Lewis, S. Salvagno, and C. J. Stirling, "Estimation of Group Dipole Moments from Surface Potential Measurements on Langmuir Monolayers",*J. Chem. Soc., Far. Trans. I*, **85**, 1009 (1989).
55. J. E. Huheey, *Inorganic Chemistry: Principles of Structure and Reactivity*, Harper & Row, New York, 1983.
56. J. March, *Advanced Organic Chemistry*, John Wiley & Sons, New York, 1985.
57. E. Grunwald, "Linear Free energy relationships: A historical perspective",*Chemtech*, **14**, 698 (1984).
58. S. Bastide, personal communication, 1996.
59. D. R. Lide ed.,The handbook of physics and chemistry, CRC Press, Boca Raton, Florida, 1992.
60. C. Hansch, A. Leo, and R. W. Taft, "A survey of Hammett Substituent Constants and resonance and field parameters",*Chem. Rev.*, **91**, 165 (1991).

Appendix 1: FTIR operation:

a.1.1 Technical considerations for FTIR:

The signal to noise ratio (SNR) depends on both spectrum resolution ($\Delta\nu$) and measurement time (T):

$$SNR \propto \Delta\nu \cdot T^{1/2} \qquad \text{(a.1.1}$$

The time is a function of the number of scans, and scanning velocity, which is usually dictated by the type of detector (Mercury Cadmium Telluride, MCT, is a fast detector while Deutterated TriGlycine Sulfate, DGTS, is a slow one). The SNR is improved at the cost of resolution (larger step, $\Delta\nu$), but lowering the resolution is limited by the width of the peaks and separation between them. For example, in my measurements, to get a detailed spectrum of a well covered surface, I improved the resolution ($\Delta\nu$ = 2 cm^{-1}) at the expense of the sensitivity, while for isotherm measurements with very low coverage I was less interested in the resolution of small details ($\Delta\nu$ = 4 cm^{-1}), and more interested in high sensitivity and good SNR in reasonable measuring time.

The electronic and digitization systems of the FTIR introduce other sources of noise, and tools to reduce them. A variety of mathematical functions are available. However, with all of them, suppressing the noise naturally reduces the resolution.

a.1.2 The FTIR operation conditions:

A DTGS (Deuterated triglycine sulfate) thermal detector was used with scanning velocity of 5 kHz and 50 scans per spectrum. The beam aperture was 12 mm and the resolution was 4 cm^{-1} for isotherm spectra, and 2 cm^{-1} for others. The intensity of the signal was 4000-6000 readings for the background.

The digitization functions include: gain switch in 300 points window, low pass filter at 16 kHz, Mertz function for phase correction, 4 points apodization function, and zero filling with factor 2. Some of these functions were chosen arbitrarily.

Appendix 2: Calculations of surface coverage and Langmuir isotherms from FTIR spectra.

1. The raw data are composed of a set of **n** IR spectra for different solution concentration (C).
2. Improving signal to noise ratio was done by Lorenzian deconvolution with a deconvolution factor of 100 and noise suppression ratio of 0.2.
3. The absorbance ($A_{c\nu}$) at specific wavenumber (ν) was calculated by integrating the peak area, for each concentration (C) spectrum.
4. The absorbance signal is related to the surface concentration (θ) by the absorptivity (a_ν) and a background contribution (b_ν): $A_{c\nu} = a_\nu \cdot \theta_c + b_\nu$. The absorptivity also includes a normalization factor that relates the number of molecules per surface area to one monolayer. Therefore we regard the θ values as fraction of a monolayer, and all the curves are normalized so as to give as highest experimental $\theta = 1$.
5. The following equations were used to evaluate the parameters for each absorbing band:

$$A_{2\nu} - A_{1\nu} = \left(a_\nu \cdot \theta_2 + b_\nu\right) - \left(a_\nu \cdot \theta_1 + b_\nu\right) = a_\nu \cdot \left(\theta_2 - \theta_1\right) \qquad \text{(a.2.1)}$$

$$\sum_c A_{c1} = a_1 \cdot \sum_c \theta_c + n b_1 \Rightarrow \frac{n b_1}{a_1} = \frac{1}{a_1} \cdot \sum_c A_{c1} - \sum_c \theta_c \qquad \text{(a.2.2)}$$

6. Using equation (a.2.1) for different bands and then dividing, gives the ratio between the different absorptivities (a_ν), and one parameter (a_1) was arbitrarily chosen as 1.

$$\frac{A_{21} - A_{11}}{A_{22} - A_{12}} = \frac{a_1 \cdot \left(\theta_2 - \theta_1\right)}{a_2 \cdot \left(\theta_2 - \theta_1\right)} = \frac{a_1}{a_2} \qquad \text{(a.2.3)}$$

7. The approximated a_ν parameters were used to calculate equation (a.2.2). The results obtained for different absorption bands were then subtracted, to get the background component (b_ν). Also here one of the bands was arbitrary chosen to have zero background contribution (b_1=0).

$$n \cdot \left(\frac{b_1}{a_1} - \frac{b_2}{a_2} \right) = \left(\frac{1}{a_1} \cdot \sum_c A_{c1} - \sum_c \theta_c \right) - \left(\frac{1}{a_2} \cdot \sum_c A_{c2} - \sum_c \theta_c \right) = \frac{1}{a_1} \cdot \sum_c A_{c1} - \frac{1}{a_2} \cdot \sum_c A_{c2} \qquad \text{(a.2.4)}$$

8. The set of data is much larger than the number of unknown parameters. Using different data will give different parameters, and different coverage (θ). Therefore, the parameter values calculated according to eqns. a.2.3 and a.2.4 were further improved by trial and error to reduce the error between coverage (θ), as calculated from different absorbance peaks (ν). The following equations were used, until an error in the calculated coverage of ~5% was achieved ($*$ means the next calculated value).

$$a_1^* = \left\langle \frac{A_{c1} - b_1}{\theta_c} \right\rangle_c \qquad \text{(a.2.5)}$$

$$b_1^* = \left\langle A_{c1} - a_1^* \cdot \theta_c \right\rangle_c \qquad \text{(a.2.6)}$$

9. An absolute experimental coverage was found by fitting the data with a two parameters function:

$C = \frac{m_1 \cdot \theta}{(1 - m_2 \cdot \theta)^2}$, where $m_1 = 1/K\theta_o$ and $m_2 = 1/\theta_o$, according to double site Langmuir isotherm. For single site isotherm, θ_o is found from the factor required to make the intercept equal 1.

Appendix 3: Theoretical calculation of Dipole moment:

3.1. Theoretical calculation based on polarizability:

- Calculating the expected change in electron affinity can be done according to Mønch[4] as follows (eq. 1.3): $\Delta\Phi = \pm\frac{1}{\varepsilon_o}\cdot\frac{p_\perp \cdot N_{ad}}{1+9\alpha_{ad}N_{ad}^{3/2}}$
- The change in dipole moment ΔP for the range of substituents used is about 5 D (table 4). The factor to convert Debye units to SI units is: 1[D] = $3.336\cdot10^{-30}$ [C·m]. To start we take the ligands to be normal to the surface, i.e. $\cos(\theta)=1$ and $\Delta P_\perp=\Delta P$.
- The polarizability of the adsorbate (α_{ad}) is estimated from the polarizability of ethyl benzoate α = 16.9 10^{-24} [cm^3] or that of benzoic acid α = 15 10^{-24} [cm^3][59] (see tables 3, 4 below). For the whole molecule it will be twice, $\alpha \geq 34\ 10^{-24}$ [cm^3]. A higher estimation for α can come when we consider the adsorbate as a metal - organic species, in which case $\alpha \geq 60\ 10^{-24}$ [cm^3].
- The surface area per molecule was measured by Dr. Stephane Bastide[58] to be $N_{ad} \approx (40_{..}^{2}.)^{-1}$ for di-carboxylic acids.

  This measurement was done on water, but can be regarded as good estimate for the surface area on the surface of a semiconductor.
- The vacuum permitivity is: ε_o = 8.854 10^{-12} [F/m].
- Inserting all values in equation 1.3 results in:

$$\Delta\Phi = \pm\frac{1}{8.854\cdot10^{-12}\left[\frac{F}{m}\right]}\cdot\frac{5\cdot\left(3.336\cdot10^{-30}\right)[C\cdot m]\cdot\left(40\cdot10^{-20}\left[m^2\right]\right)^{-1}}{1+9\cdot\left(34\cdot10^{-30}\right)\left[m^3\right]\cdot\left(40\cdot10^{-20}\left[cm^2\right]\right)^{-3/2}} \qquad \text{(a.3.1}$$

$$= \frac{4.71[V]}{1+1.21} = 2.13[V]$$

- The calculated change is $\Delta\Phi$ = 2.13 V -1.5 V for α = 34 and 60 10^{-24} [cm^3], respectively. These values are 3 - 2 times bigger than the experimental value of $\Delta\Phi \approx 0.7$ V (fig. 10).

3.2. Calculating the 'experimental' tilt:

Assuming the lower effective dipole is only due to the tilt of the molecules, we get:

$$\Delta\Phi = \Delta\Phi' \cdot \cos(\theta) \Rightarrow \theta = \cos^{-1}\left(\frac{\Delta\Phi}{\Delta\Phi'}\right) = \cos^{-1}\left(\frac{0.7}{2.13}\right) = 71^\circ \qquad \text{(a.3.2}$$

where $\Delta\Phi$ is the experimental change in EA, and $\Delta\Phi$' is the theoretical change calculated in eq. a.3.1. If we use the metal complex polarizability, the calculated tilt is only 62°.

3.3. Calculating the 'experimental' permittivity:

In this case we assume the total decrease in EA is due to average film permittivity as suggested by Oliveira et.al.[54]. Therefore:

$$\Delta\Phi = \pm\frac{1}{\varepsilon_o}\cdot\frac{p_\perp \cdot N_{ad}}{\varepsilon} \Rightarrow \varepsilon = \frac{1}{\varepsilon_o}\cdot\frac{p_\perp \cdot N_{ad}}{\Delta\Phi} = \frac{4.71[V]}{0.7[V]} = 6.73 \qquad \text{(a.3.3}$$

Here, as well, we use $\Delta\Phi$ as the experimental change in EA.

We can also relate the experimental permittivity to molecular polarizability as follows:

$$\varepsilon = 1 + 9\alpha_{ad} N_{ad}^{3/2} \Rightarrow \alpha_{ad} = \frac{\varepsilon - 1}{9N_{ad}^{3/2}} = \frac{6.73 - 1}{9/\left(40\cdot 10^{-16}\right)^{1.5}} = 161\cdot 10^{-24}\left[cm^3\right] \qquad \text{(a.3.4}$$

If we assume the tilt to be as with DS adsorption on Au[26], $\theta = 50^\circ$ than the calculated permitivity is reduced to 4.33, and the resulting polarizability is α = 93 10^{-24} [cm^3] which is closer to metal compound values.

3.4. Experimental dipole shift:

The change in electron affinity ($\Delta\chi$, fig. 10) can be fitted to changes in dipole moment (p) according to:

$$\Delta\chi = 78\cdot p + 445 \Rightarrow p_{\Delta\chi=0} = -\frac{445}{78} = -5.7D \qquad \text{for DS} \qquad \text{(a.3.6}$$

$$\Delta\chi = 114\cdot p + 466 \Rightarrow p_{\Delta\chi=0} = -\frac{466}{114} = -4.1D \qquad \text{for DC} \qquad \text{(a.3.7}$$

3.5. Expected bond-induced dipole:

The percent ionic character (I) between two elements can be approximated by the electronegativity difference (ΔEN) between them:

$$I = 16 \cdot (\Delta EN) + 3.5 \cdot (\Delta EN)^2 \qquad \text{(a.3.8}$$

The bond-induced dipole is therefore the percent of charge ($I \cdot q_e$) multiplied by the characteristic distance, which is the bond length (r):

$$p = I \cdot q_e \cdot r = I[\%] \cdot 1.6 \cdot 10^{-19}[C] \cdot r[A] \cdot 10^{-10}[m] \cdot \frac{1[D]}{3.34 \cdot 10^{-30}[C \cdot m]} = \qquad \text{(a.3.9}$$

$$0.0479 \cdot I[\%] \cdot r[A]$$

where the electronic charge, q_e=1.6·10^{-19} C, and the bond length can be estimated from ionic radii data of the elements. The required data are summarized in table 3 below.

Table 3: Chemical properties of the bonding elements (S; O; Ga; and As).

All data were taken from Huheey[55]

Element(s)	Ionic radii [Å]	Electronegativity [Pauling units]		
O^{-2}	1.22	3.44		
O^{-2} (sp^2)	1.22	5.54		
S^{-2}	1.84	2.58		
S^{-2} (sp^2)	1.84	3.21		
Ga^{+3}	0.61	2.10		
As^{+5}	0.48	2.58		
	Σ radii [Å]	ΔEN	Ionic percent - I	Induced dipole [D]
O - Ga	1.83	1.34	28	2.4
O - As	1.7	0.86	16	1.3
O(sp^2) - Ga	1.83	1.34	96	8.5
O(sp^2) - As	1.7	0.86	78	6.4
S - Ga	2.45	0.46	8.5	1.0
S - As	2.32	0	0	0
S(sp^2) - Ga	2.45	0.46	22	2.6
S(sp^2) - As	2.32	0	11	1.3

Appendix 4. Molecular parameter data

Table 4: Molecular parameter data for substituted benzene:

Name	Formula	Dipole[59] [D]	α[59] [10^{-24} cm^3]	IP[59] [eV]	Hammett parameters[60]						
					σ_p	F	R	$+\sigma_p$	$-\sigma_p$	+R	-R
CN	C_7H_5N	4.18	12.5	9.62	0.66	0.51	0.15	0.66	1	0.15	0.49
CF3	$C_7H_5F_3$	2.86		9.685	0.54	0.38	0.16	0.61	0.65	0.23	0.27
H	C_6H_6	0	10.32	9.2459	0	0.03	0	0	0	0	0
Me	C_7H_8	-0.43	12.3	8.82	-0.17	0.01	-0.18	-0.31	-0.17	-0.32	-0.18
OMe	C_7H_8O	-1.38	13.1	8.21	-0.27	0.29	-0.56	-0.78	-0.26	-1.07	-0.55
NMe2	$C_8H_{11}N$	-1.41	16.2	7.12	-0.83	0.15	-0.98	-1.7	-0.12	-1.85	-0.27
Alkyl	*	0	$\approx$40	$\approx$9.2	-0.18	-0.01	-0.2	-0.29	-0.19	-0.28	-0.18

* No values were found for C15 alkyl chain. The given values were extrapolated from values for lower carbon chains.

Table 5: Estimation of molecular parameters for the binding groups:

Name	Formula	α [10^{-24} cm^3]	IP [eV]
Alkyl chain ($C_{15}H_{32}$)			
C6	C_6H_{14}	11.9	
C7	C_7H_{16}	13.7	
C8	C_8H_{18}	19.8	9.82
C9	C_9H_{20}		9.72
C10	$C_{10}H_{22}$		9.65
C11	$C_{11}H_{24}$		9.56
anthracene	$C_{14}H_{10}$	25.4	
Di-thiane ($C_4H_8S_2$ - cyclic)			
thiacyclo hexane	$C_5H_{10}S$		8.2
diethyl disulfide	$C_4H_{10}S_2$		$\leq$ 8.27
ethyl sulfide	$C_4H_{10}S$	10.8	
Thiophene	C_4H_4S	9.67	
Tartaric acid $(CHOH)_2{\cdot}(COOH)_2$			
benzoic acid	$C_7H_6O_2$		9.47
diMe oxalate	$C_4H_6O_4$		10.0
Et. benzoate	$C_9H_{10}O_2$	16.9	
Al acetylacetonate	$C_{15}H_{21}AlO_6$	51.9	
Fe acetylacetonate	$C_{15}H_{21}FeO_6$	58.1	
Th acetylacetonate	$C_{20}H_{18}O_8Th$	79	

Appendix 5. Coverage data of di-sulfide on Gold

Data were kindly given by Urs Krops, from the organic chemistry dept., WIS.

Table 6: Coverage of di-sulfide on Au

Name	Coverage (Electrochemical potential)	Thickness (Ellipsometry) in Å
DCDS	10.9	75%
MCDS	14.7	100%
DODS	9.3	84%
MODS	14.5	94%
DFDS	9.4	94%

Appendix 6. Physical properties of clean GaAs(100) surfaces, measured by Chen et. al.

Data were measured at room temperature under UHV, for MBE, 1μm thick n-type GaAs(100). Different reconstructions are achieved for the same sample by annealing to different temperatures in As environment[50].

Table 7: Position of Fermi level, work function and ionization potential of differently reconstructed GaAs(100) surfaces.

Physical property [eV]	c(8′2)/ 4′2 Ga rich	c(4′4) Highly As rich	c(2′8)/ 2′4 As rich
$(E_C\text{-}E_F)_S$ *	0.72	0.62 - 0.72	0.68 - 0.72
$\Delta\Phi$ **	0.1	0.25	0.5
EA **	3.86	4.01	4.26

* The convention is to use $(E_F\text{-}E_v)_S$ to describe this value. For the highly doped n-type samples used in my work, we can assume BB = $(E_Cs\text{-}E_Cb) \approx (E_C\text{-}E_F)_S$. Therefore I calculated

$(E_C\text{-}E_F)_S$ = 1.42 eV - $(E_F\text{-}E_V)_S$, where 1.42 is the band gap.

** Electron affinity (EA) deduced from the original data, according to EA = Φ - $(E_C\text{-}E_F)_S$.

Appendix 7: Computer program to colect KP data with time

Program was originally written by Dr. Leonid Chernyak and modified by me.

```
//------------------------------- Libraries ----------------------
#include <dos.h>
#include <stdio.h>
#include "ieee-cpp.h"
#include <stdlib.h>
#define adr 20
#define IEEE_CONTROLER 21
#include <graphics.h>
#include <conio.h>
#include <bios.h>
//---------------------------------Time counter-------------------------------
float time(void)
// one hour timer with 0.01 sec accuracy.
{       struct  time t;
        float sec;
        gettime(&t);
        sec=float(t.ti_min)*60+float(t.ti_sec)+float(t.ti_hund)*0.01;
        return sec;     }
//-----------------------------------------------------------------------------
void main()
{
//------------------------------- Initializaton of IEEE ----------------------
{       unsigned status;
        status = gpib_board_present();
        if (status == 0)
        {       putchar ('\7');
                printf ("\n\n NO GPIB PRESENT ! \n\n");
                exit(0);            }
        initialize (IEEE_CONTROLER, 0);
        printf ("IEEE board is initionalized\n");               }
```

```
//------------------Declaring variabels---------------------------------------
        int status, l, k, color;
        char str[80], str2[83],*remark, hui, FileName[30];
        float BeginSecond, EndSecond, CarSecond, x, y, Vmin, Vmax, str1;
        float TotSecond, Screenzero, periodicity,MStime, Nsec;
        struct  time tt;
//------------------Asking parameters from user---------------------------------
        FILE *fout;
        str2[0]=81;
                        printf("File output name:");
                        scanf("%12s", FileName);
                        if((fout = fopen(FileName, "wt+"))==NULL)        // Check open a file.
                              printf ("Cann't open out file \n"), exit(0);
                        printf("Enter general text up to 80 char: \n");
                        remark=cgets(str);
                        if(fprintf(fout, "%s   \n", remark)<4)                  // writing remark to file
                             printf("Unable write to file \n"), exit(0);        //Check sucsses writing.
                        EndSecond=600.0;
                        periodicity = 5.0;                      // Time delay between two data points
                        printf("\nVmax [V]:");                          // Upper and lower voltage axis.
                        scanf("%f",&Vmax);
                        printf("Vmin [V]:");
                        scanf("%f",&Vmin);
                        TotSecond=20000*periodicity;
                        gettime(&tt);               // Calculating when (hour) will time limit reached.
                        l=int(TotSecond/3600);
                        k=l + int(tt.ti_hour);
                        l=int(tt.ti_min)+ int((TotSecond-3600*l)/60);
                        if (l>60) l=l-60, k=k+1;
                        if (k>24) k=k-24;
//-----------------------Initialization of graphics-----------------------------
/* request autodetection */
        int gdriver = DETECT, gmode;
                /* initialize graphics and local variables */
        initgraph(&gdriver, &gmode, "");
```

```
// ----------------Coordinate system-----------------------------------------
        printf("File: %s, Interval: %4.1f sec. Until: %i:%2.0i. \n",
                        FileName, periodicity, k, l);
        printf("'q' - stop, 'p' - pause, 'l'-slow, 'h'-fast \n");
        setcolor (15);                          // white color, drawing bold graph frame.
        line(100,450,600,450);
        line(100,100,100,450);
        line(600,450,600,100);
        line(100,100,600,100);
        if ((Vmin<0)&&(Vmax>0))                 // Drawing zero line if there is one.
                {       y=450+350*(Vmin-0.0)/(Vmax-Vmin);
                        line(100,y,600,y);
                        outtextxy(55,y-5,"0.0");        }
        setlinestyle(3,1,1);                                    // Dashed line for grid.
        for(k=2;k<=5;k++)                                       // Drawing vertical grid.
        line(k*100,450,k*100,100);
        for(k=1;k<=5;k++)                                       //Drawing horizontal grid.
        line(100,(450-k*70),600,(450-k*70));
        for(k=0;k<=5;k++)                                       // Writing Y-voltage labels.
        sprintf(str2,"%1.3f",Vmax+k*(Vmin-Vmax)/5),
        outtextxy(45,95+k*70,str2);
        for(k=0;k<=5;k++)                                       // Writing X-time labels.
        sprintf(str2,"%4.2f",k*EndSecond/5),
        outtextxy(85+k*100,460,str2);
//--------------------Initiate variabels-----------------------------------------// All time variabels are in sec.
        color=4;                        // red
        setcolor (color);
        CarSecond=0.0;                  // Accumulate sec. since meas begins.
        BeginSecond =time();                    // Real time for global start point.
        Screenzero=BeginSecond;                 // Real time for screen start point.
        Nsec=BeginSecond;                       // Real time for next data point.
//------------------Measurement-----------------------------------------------
while(CarSecond<TotSecond)   // Absolute time limit.
{       MStime=time();          // Reading time (sec) by time function.
        if ((Nsec-0.025)<MStime) // Only if it reached the interval data recorded.
```

```
//-------------One data point--------------------
                {       send(adr,":form:elem read",&status);
                        send(adr,":fetc?",&status); // Calling for data
                        enter(str, 80, &l, adr, &status);  // Reading data
                        CarSecond=MStime-BeginSecond; // taking time
                        fprintf (fout, "%f  %s   \n", CarSecond, str); // output to the file
                        sscanf(str, "%f", &str1); // Reading of data from the string
                        Nsec=Nsec+periodicity;      // Determining next meas. time

                        y=450+350*(Vmin-str1)/(Vmax-Vmin);       // Drawing a dot on screen
                        x=100+500*(MStime-Screenzero)/EndSecond;
                        circle(x,y,1);
                        for(l=0;l<81;l++) str[l]=0; // cleaning up the string
                        }
//-------------Check for screen end--------------------
                if (MStime>(Screenzero+EndSecond+0.05))
                        {  Screenzero=time();              // Null relative screen time.
                                color=color+1;                 // Change color.
                                if (color>=15) color=1;
                                setcolor (color);
                                sprintf(str2,"%4.0f",MStime-BeginSecond);
                                outtextxy(75,y,str2);       // Print the absolute time for new line
                        }
//-------------Check for change of hour -----------------
                if(MStime<Screenzero)
                {       Nsec=Nsec-3600.0;                    // Reduce 3602 to 2 sec for next data.
                        BeginSecond=BeginSecond-3600.0;  // Add an hour to start reference.
                        Screenzero=Screenzero-3600.0;   // Change relative screen reference.
                        }
```

```
//-------------Check for user interaction--------
                    if(bioskey(1)!=0)
                    {       hui=getch();
                            if((hui=='q')||(hui=='Q')) exit(0);                    // q to exit program.
                            if ((hui=='h')||(hui=='H'))  periodicity = 0.1;
                            if ((hui=='l')||(hui=='L'))   periodicity = 5.0;
                            if((hui=='p')||(hui=='P'))                             // p to hold the program.
                            {  Mstime=time();                                      // Record holding time.
                            printf("Program on hold. Press any key to continue. \r");
                            hui=getch();              // Wait for user reply.
                            if((hui=='q')||(hui=='Q')) CarSecond=TotSecond, exit(0);
                            printf("                                    \r");
                            MStime=time()-MStime;                          // Calculate holding period.
                            Nsec=Nsec+MStime;                                      // Add it to next meas.
                            Screenzero=Screenzero+MStime;  // Add it to screen time.
                            if (MStime<0.0)
                            BeginSecond=BeginSecond-3600.0,                // Correction if hour turn
                            MStime=MStime+3600.0;                                  // during pause.
                            TotSecond=TotSecond+MStime;                   // Add pause to final limit.
// On screen meas. continue from same point. To the file it write the real time passed (no change in
BeginSecond).
} } } }
```